



DYNAMIC SYSTEMS AND SIMULATIONS

LABORATORY

Department of Production Engineering &

Management

Technical University of Crete

**Minimization of Fuel Consumption for Vehicle
Trajectories**

by

Panagiotis Typaldos

supervisor

Prof. Ioannis Papamichail

Chania, Greece

June, 2017

Thanks

Finalizing this thesis, I would like to thank my supervisor, Prof. Ioannis Papamichail, as well as Prof. Markos Papageorgiou for all their help, guidance and continuous support during the development of this work. Most of all, I would like to thank my family for their unconditional support and encouragement all these years.

Acknowledgement

The research leading to these results has received funding partially from the European Research Council under the European Union's Seventh Framework Programme (FP/2007-2013) / ERC Grant Agreement n. [321132], project TRAMAN21 and partially from the European Commission under the European Union's Seventh Framework Programme (FP/2007-2013) / FP7-ICT-2013.3.4, project LOCAL4GLOBAL (n.611538).

Contents

	Page
1 Introduction	1
2 Theoretical Background	4
2.1 Taylor's Theorem	4
2.1.1 Taylor's Theorem for Many Variables	4
2.2 The Theory of Continuous-Time Optimal Control	6
2.2.1 Optimal Control Problem	6
2.3 The Theory of Discrete-Time Optimal Control	8
2.3.1 Problem Formulation	8
2.3.2 Optimality Conditions	9
2.4 Feasible Direction Algorithm	11
2.4.1 Reduced Gradient	11
2.4.2 Basic Algorithmic Structure	13
2.4.3 Specification of a Search Direction	14
2.4.4 Constant Control Bounds	18
2.5 ARRB Fuel Consumption Model	19
2.6 Smoothing Function	23
3 Description of the problem	26
3.1 Taylor Approximation of the Fuel Consumption Model	28
3.2 Optimal Control Methodology	28
4 Results	33
4.1 Analytic Solution of Taylor Approximation	33
4.2 A Numerical Solution of the Fuel Consumption Model	37
4.2.1 Piecewise Constant Solution	39
4.2.2 Piecewise Linear Interpolation Solution	41
4.3 Feasible Direction Algorithm	44

4.4	Fuel Consumption Comparison for Different Time Step and Same Time Horizon Cases	51
4.5	Fuel Consumption Comparison for the Same Time Step and Different Time Horizon Cases	53
5	Comparison Between Analytic Solution of Fuel Consumption's Model Approximation and Numerical Solutions	61
6	Maximisation Problem	67
7	Conclusions	71
	References	73

List of Figures

1	A 3D representation of ARRB Fuel Consumption Model, instantaneous fuel consumption	25
2	A 2D representation (assuming that the value of speed is constant, $v = 15$ m/s) of ARRB Fuel Consumption Model, instantaneous fuel consumption and the smoothed model for different values of α_s	25
3	The positions of the "EGO" vehicle and its putative leader at the beginning and the end of the merging procedure.	26
4	Graphical representation of the optimal solution, regarding the minimisation of the approximated fuel consumption model for scenario 1.	34
5	Graphical representation of the optimal solution, regarding the minimisation of the approximated fuel consumption model for scenario 2.	34
6	Graphical representation of the optimal solution, regarding the minimisation of the approximated fuel consumption model for scenario 3.	35
7	Graphical representation of the optimal solution, regarding the minimisation of the approximated fuel consumption model for scenario 4.	35
8	Graphical representation of the optimal solution, regarding the minimisation of the approximated fuel consumption model for scenario 5.	36
9	Flow Chart	38
10	Control and states diagrams for the Piecewise-Constant solution for Scenario 1	39
11	Control and states diagrams for the Piecewise-Constant solution for Scenario 2	39
12	Control and states diagrams for the Piecewise-Constant solution for Scenario 3	40
13	Control and states diagrams for the Piecewise-Constant solution for Scenario 4	40

14	Control and states diagrams for the Piecewise-Constant solution for Scenario 5	41
15	Control and states diagrams for the Piecewise-Linear solution for Scenario 1	41
16	Control and states diagrams for the Piecewise-Linear solution for Scenario 2	42
17	Control and states diagrams for the Piecewise-Linear solution for Scenario 3	42
18	Control and states diagrams for the Piecewise-Linear solution for Scenario 4	43
19	Control and states diagrams for the Piecewise-Linear solution for Scenario 5	43
20	Objective function decrease in dependence of the computing time and evolution of control and states, in dependence of the number of time steps for Scenario 1	46
21	Objective function decrease in dependence of the computing time and evolution of control and states, in dependence of the number of time steps for Scenario 2	47
22	Objective function decrease in dependence of the computing time and evolution of control and states, in dependence of the number of time steps for Scenario 4	49
23	Objective function decrease in dependence of the computing time and evolution of control and states, in dependence of the number of time steps for Scenario 5	50
24	Controls and states of the analytic solution of the approximated fuel consumption model and the smoothed fuel consumption model for the case of $T = 19s$ and $KMAX=100$ for Scenario 1	53
25	Controls and states of the analytic solution of the approximated fuel consumption model and the smoothed fuel consumption model for the case of $T = 38s$ and $KMAX=200$ for Scenario 1	54
26	Controls and states of the analytic solution of the approximated fuel consumption model and the smoothed fuel consumption model for the case of $T = 57s$ and $KMAX=300$ for Scenario 1	54
27	Controls and states of the analytic solution of the approximated fuel consumption model and the smoothed fuel consumption model for the case of $T = 19s$ and $KMAX=100$ for Scenario 2	55
28	Controls and states of the analytic solution of the approximated fuel consumption model and the smoothed fuel consumption model for the case of $T = 38s$ and $KMAX=200$ for Scenario 2	55

29	Controls and states of the analytic solution of the approximated fuel consumption model and the smoothed fuel consumption model for the case of $T = 57s$ and $KMAX=300$ for Scenario 2	56
30	Controls and states of the analytic solution of the approximated fuel consumption model and the smoothed fuel consumption model for the case of $T = 15.5s$ and $KMAX=100$ for Scenario 3	56
31	Controls and states of the analytic solution of the approximated fuel consumption model and the smoothed fuel consumption model for the case of $T = 31s$ and $KMAX=200$ for Scenario 3	57
32	Controls and states of the analytic solution of the approximated fuel consumption model and the smoothed fuel consumption model for the case of $T = 46.5s$ and $KMAX=300$ for Scenario 3	57
33	Controls and states of the analytic solution of the approximated fuel consumption model and the smoothed fuel consumption model for the case of $T = 25s$ and $KMAX=100$ for Scenario 4	58
34	Controls and states of the analytic solution of the approximated fuel consumption model and the smoothed fuel consumption model for the case of $T = 50s$ and $KMAX=200$ for Scenario 4	58
35	Controls and states of the analytic solution of the approximated fuel consumption model and the smoothed fuel consumption model for the case of $T = 75s$ and $KMAX=300$ for Scenario 4	59
36	Controls and states of the analytic solution of the approximated fuel consumption model and the smoothed fuel consumption model for the case of $T = 25s$ and $KMAX=100$ for Scenario 5	59
37	Controls and states of the analytic solution of the approximated fuel consumption model and the smoothed fuel consumption model for the case of $T = 50s$ and $KMAX=200$ for Scenario 5	60
38	Controls and states of the analytic solution of the approximated fuel consumption model and the smoothed fuel consumption model for the case of $T = 75s$ and $KMAX=300$ for Scenario 5	60
39	Comparison of control and states of analytic Solution of $\frac{1}{2}u^2$, smoothed function of ARRB fuel consumption model, Analytic Solution of the approximated model and piecewise constant method for Scenario 1	62

40	Comparison of control and states of analytic Solution of $\frac{1}{2}u^2$, smoothed function of ARRB fuel consumption model, Analytic Solution of the approximated model and piecewise constant method for Scenario 2	63
41	Comparison of control and states of analytic Solution of $\frac{1}{2}u^2$, smoothed function of ARRB fuel consumption model, Analytic Solution of the approximated model and piecewise constant method for Scenario 3	64
42	Comparison of control and states of analytic Solution of $\frac{1}{2}u^2$, smoothed function of ARRB fuel consumption model, Analytic Solution of the approximated model and piecewise constant method for Scenario 4	65
43	Comparison of control and states of analytic Solution of $\frac{1}{2}u^2$, smoothed function of ARRB fuel consumption model, Analytic Solution of the approximated model and piecewise constant method for Scenario 5	66
44	Comparison between minimisation and maximisation problem of the smoothed fuel consumption model for Scenario 1	68
45	Comparison between minimisation and maximisation problem of the smoothed fuel consumption model for Scenario 3	69
46	Comparison between minimisation and maximisation problem of the smoothed fuel consumption model for Scenario 4	70

List of Tables

1	Comparison of search direction methods for Scenario 1	45
2	Comparison of search direction methods for Scenario 2	45
3	Comparison of search direction methods for Scenario 4	48
4	Comparison of search direction methods for Scenario 5	48
5	Fuel Consumption based on the ARRB fuel consumption model for the same time horizon situation and different number of time steps for the scenario 1	51
6	Fuel Consumption based on the ARRB fuel consumption model for the same time horizon situation and different number of time steps for the scenario 2	52
7	Fuel Consumption based on the ARRB fuel consumption model for the same time horizon situation and different number of time steps for the scenario 3	52
8	Fuel Consumption based on the ARRB fuel consumption model for the same time horizon situation and different number of time steps for the scenario 4	52
9	Fuel Consumption based on the ARRB fuel consumption model for the same time horizon situation and different number of time steps for the scenario 5	52
10	Optimal fuel consumption of analytic solution of $\frac{1}{2}u^2$, smoothed function, analytic solution of the approximated model and piecewise constant method for Scenario 1	62
11	Optimal fuel consumption of analytic solution of $\frac{1}{2}u^2$, smoothed function, analytic solution of the approximated model and piecewise constant method for Scenario 2	63
12	Optimal fuel consumption of analytic solution of $\frac{1}{2}u^2$, smoothed function, analytic solution of the approximated model and piecewise constant method for Scenario 3	64
13	Optimal fuel consumption of analytic solution of $\frac{1}{2}u^2$, smoothed function, analytic solution of the approximated model and piecewise constant method for Scenario 4	65

14	Optimal fuel consumption of analytic solution of $\frac{1}{2}u^2$, smoothed function, analytic solution of the approximated model and piecewise constant method for Scenario 5	66
15	Maximum and minimum fuel consumption values of the smoothed fuel consumption model for scenario 1	68
16	Maximum and minimum fuel consumption values of the smoothed fuel consumption model for scenario 3	69
17	Maximum and minimum fuel consumption values of the smoothed fuel consumption model for scenario 4	70

1

Introduction

Nowadays, the energy and fuel consumption reduction is of high importance. The current trend towards increased mobility and transportation growth in the more developed countries runs counter to the purposes of controlling the greenhouse effect, local pollution and the exploitation of fuel resources. The fact that mobility is increasing and millions of new drivers start using private cars as a main mode of transportation every year, leads on an increase in the demand for primary energy, and the more fossil energy is used, the more the local emissions (unburnt hydrocarbons, carbon monoxide (CO), NO_x, particulate matter, sulfur oxide (SO_x) and volatile organic compounds (VOCs)) and the corresponding greenhouse gases emissions are increased, so fuel consumption is a crucial issue and it is carried out intensive research in order to be found an optimal solution. Research related to the idea of controlling a vehicle for improving its fuel economy has a long track. Some early studies were conducted to determine the optimal cruising velocity of a vehicle based on its internal operating characteristics (Gilbert, 1976; Chang and Morlok, 2005). In a study, the optimal values of acceleration for starting up and cruising speed over hilly terrains or flat roads were determined for fuel efficient driving (Hooker, 1988). Another available method for improving fuel economy is eco-driving and eco-routing. Ecological (eco)-driving is a way of maneuvering a vehicle with a human driver that is intended to minimize fuel consumption while coping with varying and uncertain road traffic by trading off the most efficient driving point of the vehicle whenever necessary. Aside from various physical factors, driving style has a great influence on vehicle emissions and energy consumption (Van Mierlo et al., 2004). Driving style has the capacity to significantly improve the driving efficiency of a vehicle. At present, eco-driving systems can be divided into two categories: one focuses on the entire transportation system and tries to reduce the overall fuel consumption by route optimization and traffic management and the other fo-

cuses on a single vehicle and reduces the fuel consumption by optimize the driving style of the driver and control the power management system of the vehicle. Several studies have indicated that eco-driving can improve fuel economy by 15-25% (CIECA, 2009; Hellström et al., 2009; Kamal et al., 2011; Cheng et al., 2013; Casavola et al., 2010; Kundu et al., 2013; Dhaou, 2011), and approximately 12-33% of fuel can be saved through eco-routing (Dhaou, 2011; Streets, 2009). Therefore, eco-driving and eco-routing are effective ways to improve fuel economy in both the short-term and long-term. To evaluate eco-driving and eco-routing algorithms, an appropriate fuel consumption model that can predict instantaneous fuel consumption second by second is needed. To identify the fuel consumption models that are best suited for eco-driving and eco-routing, a review of state-of-the-art fuel consumption models is necessary. Faris et al. performed a comprehensive review of state-of-the-art fuel consumption and emission models, such as the VT-Micro model (Ahn et al., 2002), power-based fuel consumption model (Post et al., 1984), and POLY model (Teng et al., 2002), and classified these models into five broad categories: (1) modeling based on the scale of the input variables, (2) modeling based on a formulation approach, (3) modeling based on the type of explanatory variables, (4) modeling based on state variable values and (5) modeling based on the number of dimensions (Faris et al., 2011).

This master thesis is composed of 6 chapters. Chapter 2 starts with a brief review of the methodologies and mathematical tools that are used in this thesis. In Chapter 3, we present the description and the formulation of the problem. Afterwards, we approximate the fuel consumption function with a quadratic function via Taylor expansion, in order to solve it analytically, using Hamiltonian analysis as in the optimal control methodology described in Chapter 2. Then we show the results of the 5 scenarios defined at the beginning of the chapter and also the results of an equivalent modified problem numerical solution as it is shown in section 4.2. Chapter 2.4, consists of a detailed description of a feasible direction algorithm (Papageorgiou and Marinaki, 1995) for the discrete-time optimal control problems which is used in order to solve the energy-based fuel consumption model minimisation problem numerically. However, because the energy-based fuel consumption model is a non-smooth function, we use a smooth model of the fuel consumption model as described in Section 2.6. Chapter 5 contains the results of the comparison of the analytic and numerical solutions of the previous chapters, in terms of the acceleration, the position, the speed trajectories and the optimal fuel consumption and also the results solving the problem described in Chapter 3 but instead of using the fuel consumption model as cost function, we use the function $f(v, a) = \frac{1}{2}a^2$, which is widely used in bibliography

as an eco-driving cost criterion. Finally, in Chapter 6, we present some results of the comparison between the results obtained from the maximisation of the cost function and the corresponding minimisation results of the problem.

2

Theoretical Background

The objective of this work is the minimisation of the fuel consumption for vehicle trajectories as it is described in Chapter 3. This is achieved by the use of optimal control theory, firstly analytically and then numerically. In order to solve the problem analytically, we need to approximate the cost function through Taylor series. As far as the numerical solution is concerned, we use a feasible direction algorithm proposed by [Papageorgiou and Marinaki \(1995\)](#). Through the optimal control methodology, we obtain the optimal trajectories of speed, position and acceleration, which then used to calculate the minimum fuel consumption. The fuel consumption model used for the estimation of the vehicle's fuel consumption rate, is the energy-related model proposed in [Post et al. \(1984\)](#). The methodologies and the mathematical tools are described in the following sections.

2.1 Taylor's Theorem

Taylor's theorem is a central tool for finding accurate numerical approximations of functions, and as such plays an important role in many areas of applied and computational mathematics. The strategy used to prove Taylor's theorem is to reduce it to the one-variable case by probing a function of many variables along lines of the form $\mathbf{I}(t) = \mathbf{x}_0 + t\mathbf{h}$ emanating from a point \mathbf{x}_0 and heading in the direction \mathbf{h} ([Marsden and Tromba, 1996](#)).

2.1.1 Taylor's Theorem for Many Variables

If $f : \mathbb{R}^n \rightarrow \mathbb{R}$ is differentiable at \mathbf{x}_0 and we define

$$R_1(\mathbf{x}_0, \mathbf{h}) = f(\mathbf{x}_0 + \mathbf{h}) - f(\mathbf{x}_0) - [\mathbf{D}f(\mathbf{x}_0)](\mathbf{h}),$$

so that

$$f(\mathbf{x}_0 + \mathbf{h}) = f(\mathbf{x}_0) + [\mathbf{D}f(\mathbf{x}_0)](\mathbf{h}) + R_1(\mathbf{x}_0, \mathbf{h}),$$

then by definition of differentiability,

$$\frac{|R_1(\mathbf{x}_0, \mathbf{h})|}{\|\mathbf{h}\|} \rightarrow 0 \quad \text{as } \mathbf{h} \rightarrow 0;$$

that is, $R_1(\mathbf{x}_0, \mathbf{h})$ vanishes to first order at \mathbf{x}_0 . In summary, we have:

Theorem 1 (First-Order Taylor Formula). *Let $f : U \subset \mathbb{R}^n \rightarrow \mathbb{R}$ be differentiable at $\mathbf{x}_0 \in U$. Then*

$$f(\mathbf{x}_0 + \mathbf{h}) = f(\mathbf{x}_0) + \sum_{i=1}^n h_i \frac{\partial f}{\partial x_i}(\mathbf{x}_0) + R_1(\mathbf{x}_0, \mathbf{h}),$$

where $R_1(\mathbf{x}_0, \mathbf{h})/\|\mathbf{h}\| \rightarrow 0$ as $\mathbf{h} \rightarrow \mathbf{0}$ in \mathbb{R}^n .

the second-order version is as follows:

Theorem 2 (Second-order Taylor Formula). *Let $f : U \subset \mathbb{R}^n \rightarrow \mathbb{R}$ have continuous partial derivatives of second order. Then we may write*

$$f(\mathbf{x}_0 + \mathbf{h}) = f(\mathbf{x}_0) + \sum_{i=1}^n h_i \frac{\partial f}{\partial x_i}(\mathbf{x}_0) + \frac{1}{2} \sum_{i,j=1}^n h_i h_j \frac{\partial^2 f}{\partial x_i \partial x_j}(\mathbf{x}_0) + R_2(\mathbf{x}_0, \mathbf{h}),$$

where $R_2(\mathbf{x}_0, \mathbf{h})/\|\mathbf{h}\|^2 \rightarrow 0$ as $\mathbf{h} \rightarrow \mathbf{0}$ and the second sum is over all i 's and j 's between 1 and n (so there are n^2 terms).

Notice that this result can be written in matrix form as

$$\begin{aligned}
f(\mathbf{x}_0 + \mathbf{h}) &= f(\mathbf{x}_0) + \begin{bmatrix} \frac{\partial f}{\partial x_1}, \dots, \frac{\partial f}{\partial x_n} \end{bmatrix} \begin{bmatrix} h_1 \\ \vdots \\ h_n \end{bmatrix} \\
&+ \frac{1}{2} [h_1, \dots, h_n] \begin{bmatrix} \frac{\partial^2 f}{\partial x_1 \partial x_1} & \frac{\partial^2 f}{\partial x_1 \partial x_2} & \cdots & \frac{\partial^2 f}{\partial x_1 \partial x_n} \\ \frac{\partial^2 f}{\partial x_2 \partial x_1} & \frac{\partial^2 f}{\partial x_2 \partial x_2} & \cdots & \frac{\partial^2 f}{\partial x_2 \partial x_n} \\ \vdots & & & \\ \frac{\partial^2 f}{\partial x_n \partial x_1} & \frac{\partial^2 f}{\partial x_n \partial x_2} & \cdots & \frac{\partial^2 f}{\partial x_n \partial x_n} \end{bmatrix} \begin{bmatrix} h_1 \\ h_2 \\ \vdots \\ h_n \end{bmatrix} \\
&+ R_2(\mathbf{x}_0, \mathbf{h}),
\end{aligned}$$

where the derivatives of f are evaluated at \mathbf{x}_0 .

2.2 The Theory of Continuous-Time Optimal Control

Many management science applications involve the control of dynamic systems, i.e., systems that evolve over time. They are called continuous-time systems or discrete-time systems depending on whether time varies continuously or discretely. Optimal control theory is a branch of mathematics developed to find optimal ways to control a dynamic system.

In an optimal control problem for a dynamic system, the task is finding an admissible control trajectory $u : [t_a, t_b] \rightarrow \Omega \subseteq \mathbb{R}^m$ generating the corresponding state trajectory $x : [t_a, t_b] \rightarrow \mathbb{R}^n$ such that the cost functional $J(u)$ is minimized.

2.2.1 Optimal Control Problem

Consider the minimisation of the cost function

$$J[u(t)] = \int_{t_0}^T \Phi(\mathbf{x}(t), \mathbf{u}(t), t) dt \quad (1)$$

subject to a system of n first-order ordinary differential equations

$$\dot{\mathbf{x}} = \mathbf{f}(\mathbf{x}(t), \mathbf{u}(t), t) \quad (2)$$

satisfying the boundary condition given by

$$\mathbf{x}(t_0) = \mathbf{x}_0 \quad (3)$$

$$\psi(\mathbf{x}(T), T) = 0 \quad (4)$$

Here $\mathbf{x} \in \mathbb{R}^n$ represents the state, $\mathbf{x}_0 \in \mathbb{R}^n$ is a specified initial point, $\mathbf{u} \in \mathbb{R}^m$ is the control, $t \in \mathbb{R}$ is a general time index, $t_0 \in \mathbb{R}$ is the initial time which is assumed to be fixed, $T \in \mathbb{R}$ the terminal time which may be fixed or varying, $\Phi(\mathbf{x}(t), \mathbf{u}(t), t) : \mathbb{R}^n \times \mathbb{R}^m \times \mathbb{R} \rightarrow \mathbb{R}$ is the full time performance index, $\mathbf{f}(\mathbf{x}(t), \mathbf{u}(t), t) : \mathbb{R}^n \times \mathbb{R}^m \times \mathbb{R} \rightarrow \mathbb{R}^n$ is the system dynamics and $\psi(\mathbf{x}(T), T) : \mathbb{R}^n \times \mathbb{R} \rightarrow \mathbb{R}^{p \leq n}$ a terminal time constraint. The control \mathbf{u} is constrained by the following inequalities by component:

$$|u_i| \leq u_{i0} = \text{constant}, \quad i = 1, 2, \dots, m$$

Theorem 3 (Necessary Conditions for Optimality). *Let the pre-Hamiltonian \bar{H} be defined such that*

$$\bar{H}(\mathbf{x}, \boldsymbol{\lambda}, \mathbf{u}, t) = \Phi(\mathbf{x}, \mathbf{u}, t) + \boldsymbol{\lambda}^T \mathbf{f}(\mathbf{x}, \mathbf{u}, t) \quad (5)$$

where $\boldsymbol{\lambda}$ is a costate adjoint to \mathbf{f} . Then, the Pontryagin's principle provides the following 1st order necessary conditions for optimality:

$$\dot{\mathbf{x}} = \frac{\partial \bar{H}(\mathbf{x}, \boldsymbol{\lambda}, \mathbf{u}, t)}{\partial \boldsymbol{\lambda}} \quad (6)$$

$$\dot{\boldsymbol{\lambda}} = \frac{\partial \bar{H}(\mathbf{x}, \boldsymbol{\lambda}, \mathbf{u}, t)}{\partial \mathbf{x}} \quad (7)$$

$$\mathbf{u} = \arg \min_{\mathbf{u}} \bar{H}(\mathbf{x}, \boldsymbol{\lambda}, \mathbf{u}, t) \quad (8)$$

Substituting (8) into (5), (6), and (7) results in a standard Hamiltonian system for state and costate only:

$$H(\mathbf{x}, \boldsymbol{\lambda}, t) = \bar{H}(\mathbf{x}, \boldsymbol{\lambda}, \arg \min_{\mathbf{u}} \bar{H}(\mathbf{x}, \boldsymbol{\lambda}, \mathbf{u}, t), t) \quad (9)$$

$$\dot{\mathbf{x}} = \frac{\partial H(\mathbf{x}, \boldsymbol{\lambda}, t)}{\partial \boldsymbol{\lambda}} \quad (10)$$

$$\dot{\boldsymbol{\lambda}} = \frac{\partial H(\mathbf{x}, \boldsymbol{\lambda}, t)}{\partial \mathbf{x}} \quad (11)$$

Evaluating the optimal trajectory corresponds to solving this system of ordinary differential equations (ODEs) satisfying the given boundary conditions. The initial state \mathbf{x}_0

and the terminal state \mathbf{x}_f are given explicitly and the initial costate $\boldsymbol{\lambda}_0$ and the terminal costate $\boldsymbol{\lambda}_f$ should be determined. We need to solve this system of ODEs with the same number of split boundary conditions. Hence the optimal control problem is reduced to a TPBVP of the Hamiltonian system.

2.3 The Theory of Discrete-Time Optimal Control

2.3.1 Problem Formulation

We consider a discrete-time dynamic process described by the following set of difference equations organized in vector form

$$\mathbf{x}(k+1) = \mathbf{f}[\mathbf{x}(k), \mathbf{u}(k), k], \quad k = 0, \dots, K-1 \quad (12)$$

where $\mathbf{x} \in \mathbb{R}^n$, $\mathbf{u} \in \mathbb{R}^m$ are the system state and control variable respectively, and $\mathbf{f} \in \mathbb{R}^n$ is a twice continuous differentiable vector function. Moreover, $\cdot(k)$ denotes the value of the corresponding variable at time $t = kT$, where T is the sample time interval, k is the discrete time index, and K (or $K \cdot T$) is the fixed time horizon. The system has a known initial state

$$\mathbf{x}(0) = \mathbf{x}_0. \quad (13)$$

The problem consists in minimizing the discrete-time cost function

$$J = \theta[\mathbf{x}(K)] + \sum_{k=0}^{K-1} \Phi[\mathbf{x}(k), \mathbf{u}(k), k] \quad (14)$$

subject to (12),(13), and the set of inequality constraints

$$\mathbf{h}[\mathbf{x}(k), \mathbf{u}(k), k] \leq \mathbf{0}, \quad k = 0, \dots, K-1 \quad (15)$$

where $\theta, \Phi, \mathbf{h} \in \mathbb{R}^q$ are twice continuous differentiable functions. The final state may be free or may be required to satisfy a final condition

$$\mathbf{g}[\mathbf{x}(K)] = \mathbf{0} \quad (16)$$

where $\mathbf{g} \in \mathbb{R}^l, l \leq n$, is a twice continuous differentiable vector function.

Although expressing a dynamic physical procedure, the above formulated problem is, from a mathematical point of view, a static optimization problem due to the discrete-time nature of the involved process. To see this, define the vectors

$$\mathbf{X} = [\mathbf{x}(1)^T \mathbf{x}(2)^T \dots \mathbf{x}(K)^T]^T, \quad \mathbf{U} = [\mathbf{u}(1)^T \mathbf{u}(2)^T \dots \mathbf{u}(K)^T]^T.$$

The discrete-time optimal control problem may then be expressed as follows:

$$\begin{aligned} & \text{Minimize } \Phi(\mathbf{X}, \mathbf{U}) \\ & \text{subject to} \\ & \mathbf{F}(\mathbf{X}, \mathbf{U}) = \mathbf{0}, \quad \mathbf{H}(\mathbf{x}, \mathbf{U}) \leq \mathbf{0} \end{aligned}$$

where Φ expresses the discrete-time cost function (14), \mathbf{H} the inequality constraints (15) for all $k \in [0, K - 1]$, and \mathbf{F} the state equations (12) for all $k \in [0, K - 1]$ and the terminal condition (16). In the following we will assume that the functions \mathbf{F}, \mathbf{H} satisfy the Kuhn-Tucker qualification condition (Fletcher, 2013).

2.3.2 Optimality Conditions

To derive necessary conditions of optimality we use the Lagrangian Function (see e.g. Papageorgiou et al. (1991); Fletcher (2013)) for this problem

$$\begin{aligned} L(\mathbf{x}(k), \mathbf{u}(k), \boldsymbol{\lambda}(k), \boldsymbol{\mu}(k), \mathbf{v}, k) &= \Phi(\mathbf{X}, \mathbf{U}) + \boldsymbol{\Lambda}^T \mathbf{F}(\mathbf{X}, \mathbf{U}) + \mathbf{M}^T \mathbf{H}(\mathbf{X}, \mathbf{U}) = \\ &= \theta[\mathbf{x}(K)] + \sum_{k=0}^{K-1} \Phi[\mathbf{x}(k), \mathbf{u}(k), k] + \sum_{k=0}^{K-1} \{\boldsymbol{\lambda}(k+1)^T [\mathbf{f}[\mathbf{x}(k), \mathbf{u}(k), k] - \\ &- \mathbf{x}(k+1)] + \boldsymbol{\mu}(k)^T \mathbf{h}[\mathbf{x}(k), \mathbf{u}, k]\} + \mathbf{v}^T \mathbf{g}[\mathbf{x}(K)] \end{aligned} \quad (17)$$

where $\boldsymbol{\lambda}(k+1) \in \mathbb{R}^n$ and $\boldsymbol{\mu}(k) \in \mathbb{R}^q$, $k = 0, \dots, K - 1$, are **Lagrange** and **Kuhn-Tucker multipliers** respectively, for the corresponding equality conditions and

$$\boldsymbol{\Lambda} = [\boldsymbol{\lambda}(1)^T \dots \boldsymbol{\lambda}(K)^T \mathbf{v}^T], \quad \mathbf{M} = [\boldsymbol{\mu}(0)^T \dots \boldsymbol{\mu}(K-1)^T]^T$$

The multipliers $\mathbf{v} \in \mathbb{R}^l$ are assigned to the final condition (16). Applying the necessary conditions of optimality, i.e.

$$dL/d\mathbf{X} = \mathbf{0}, \quad dL/d\mathbf{U} = \mathbf{0}, \quad dL/d\boldsymbol{\Lambda} = \mathbf{0}, \quad \mathbf{H}(\mathbf{X}, \mathbf{U}) \leq \mathbf{0}, \quad \mathbf{H}^T \mathbf{M} = \mathbf{0}, \quad \mathbf{M} \geq \mathbf{0}$$

we derive the necessary conditions of optimality for the discrete-time optimal control problem. These conditions are traditionally expressed in terms of the discrete-time **Hamiltonian Function** that is defined as follows

$$H[\mathbf{x}(k), \mathbf{u}, \boldsymbol{\lambda}(k+1), k] = \Phi[\mathbf{x}(k), \mathbf{u}(k), k] + \boldsymbol{\lambda}(k+1)^T \mathbf{f}[\mathbf{x}(k), \mathbf{u}(k), k]. \quad (18)$$

We also define the **extended** discrete-time Hamiltonian

$$\begin{aligned} \tilde{H}[\mathbf{x}(k), \mathbf{u}, \boldsymbol{\lambda}(k+1), \boldsymbol{\mu}(k), k] &= \Phi[\mathbf{x}(k), \mathbf{u}(k), k] + \boldsymbol{\lambda}(k+1)^T \mathbf{f}[\mathbf{x}(k), \mathbf{u}(k), k] + \\ &+ \boldsymbol{\mu}(k)^T \mathbf{h}[\mathbf{x}(k), \mathbf{u}(k), k]. \end{aligned} \quad (19)$$

We then have the following necessary conditions of optimality for the discrete-time optimal control problem:

There exist multipliers \mathbf{v} and $\boldsymbol{\lambda}(k+1), \boldsymbol{\mu}(k), k = 0, \dots, K-1$, such that the following equations are satisfied for $k = 0, \dots, K-1$ (notation: $x_y = dx/dy$):

$$\mathbf{x}(k+1) = \tilde{H}_{\boldsymbol{\lambda}(k+1)} = \mathbf{f}[\mathbf{x}(k), \mathbf{u}(k), k] \quad (20)$$

$$\boldsymbol{\lambda}(k) = \tilde{H}_{\mathbf{x}(k)} = \Phi_{\mathbf{x}(k)} + \mathbf{f}_{\mathbf{x}(k)}^T \boldsymbol{\lambda}(k+1) + \mathbf{h}_{\mathbf{x}(k)}^T \boldsymbol{\mu}(k) \quad (21)$$

$$\tilde{H}_{\mathbf{u}(k)} = \Phi_{\mathbf{u}(k)} + \mathbf{f}_{\mathbf{u}(k)}^T \boldsymbol{\lambda}(k+1) + \mathbf{h}_{\mathbf{u}(k)}^T \boldsymbol{\mu}(k) = 0 \quad (22)$$

$$\boldsymbol{\mu}(k)^T \mathbf{h}[\mathbf{x}(k), \mathbf{u}(k), k] = 0 \quad (23)$$

$$\boldsymbol{\mu} \geq \mathbf{0} \quad (24)$$

$$\mathbf{h}[\mathbf{x}(k), \mathbf{u}(k), k] \leq \mathbf{0}. \quad (25)$$

Moreover, the following **boundary** and **transversality conditions** must be satisfied

$$\mathbf{x}(0) = \mathbf{x}_0 \quad (26)$$

$$\mathbf{g}[\mathbf{x}(K)] = \mathbf{0} \quad (27)$$

$$\boldsymbol{\lambda}(K) = \theta_{\mathbf{x}(K)} + \mathbf{g}_{\mathbf{x}(K)}^T \mathbf{v}. \quad (28)$$

For a better understanding of these conditions we provide the following remarks:

- the conditions (20) and (21) are the **state** and **costate difference equations** respectively. Together they are referred to as the **system of canonical difference equations** of the problem.

- The conditions (22)-(25) are generally sufficient to provide $\mathbf{u}(k)$, $\boldsymbol{\mu}(k)$ in terms of $\mathbf{x}(k)$, $\boldsymbol{\lambda}(k)$, although this may be difficult analytically for complex problems. Therefore (22)-(25) may be referred to as **coupling conditions**. The coupling conditions obviously require that the extended Hamiltonian \tilde{H} at any time k have a stationary point at the corresponding control input $\mathbf{u}(k)$ subject to the constraints (15).
- The boundary and transversality conditions (26)-(28) include a total of $2n + 1$ equations. Together with the canonical difference equations and the coupling conditions they define a **discrete-time Two-Point-Boundary-Value-Problem (TPBVP)**, that requires $2n$ boundary values for its solution. The resting l boundary conditions are needed for the specification of the multipliers \mathbf{v} .
- The solution of the TPBVP may be found analytically for simple problems. More complex optimal control problems require the employment of numerical solution algorithms. One particular numerical algorithm will be presented in section 2.4.

2.4 Feasible Direction Algorithm

The analytic solution of optimal control problems by use of the necessary conditions of optimality derived from Section 2.3 is only possible for simple problems, e.g. problems with very low dimension or problems with special structure (e.g. Linear-Quadratic Optimization). In all other cases, numerical solution algorithms are required for calculation of the optimal trajectory $\mathbf{u}(k), \mathbf{x}(k + 1)$, $k = 0, \dots, K - 1$. This chapter presents a particular feasible direction algorithm that has demonstrated efficiency in a number of different applications, particularly in the case of simple inequality constraints and free final state.

2.4.1 Reduced Gradient

We first consider the simpler optimal control problem of minimizing (14) subject to (12), (13), i.e., for the time being, we consider a free final state and no inequality constraints. In this case the necessary conditions (20)-(28) are simplified as follows:

- (20), (26) remain as they are

- The third term of the r.h.s of (21), (22) may be dropped, i.e. we have

$$\boldsymbol{\lambda}(k) = H_{\mathbf{x}(k)} = \Phi_{\mathbf{x}(k)} + \mathbf{f}_{x(k)}^T \boldsymbol{\lambda}(k+1) \quad (29)$$

$$H_{\mathbf{u}(k)} = \Phi_{\mathbf{u}(k)} + \mathbf{f}_{\mathbf{u}(k)}^T \boldsymbol{\lambda}(k+1) = \mathbf{0} \quad (30)$$

- (23), (24), (25), (27) may be dropped.
- (28) is simplified as follows

$$\boldsymbol{\lambda}(K) = \theta_{\mathbf{x}(K)}. \quad (31)$$

For a given control trajectory $\mathbf{u}(k)$, $k = 0, \dots, K-1$, we may solve (12) with initial condition (13) to obtain $\mathbf{x}(k)$, $k = 1, \dots, K$. Substituting the control trajectory $\mathbf{u}(k)$ and the corresponding $\mathbf{x}(k)$ in (14), we obtain the corresponding value of the cost criterion, which therefore may be considered to depend only on $\mathbf{u}(k)$ (not on $\mathbf{x}(k)$). In other words the control variables $\mathbf{u}(k)$ may be considered as the independent optimization variables, the state variables $\mathbf{x}(k)$ being derivable from them via (12), (13). Thus setting $\mathbf{x}(k) = \mathbf{x}(\mathbf{u}(k))$, we define $\bar{J}[\mathbf{u}(k)] = J[\mathbf{x}(\mathbf{u}(k)), \mathbf{u}(k)]$. We call $d\bar{J}/d\mathbf{u}(k) = \bar{J}_{\mathbf{u}(k)}$ the **reduced gradient** of the cost function J w.r.t. the state equality constraints (12). It can be shown (Papageorgiou et al., 1991) that the reduced gradient $\bar{J}_{\mathbf{u}(k)}$ of the cost function (14) w.r.t. (13) may be calculated according to the following procedure:

- Calculation of $\mathbf{x}(k)$, $k = 1, \dots, K$, via forward integration of (12) with initial state (13).
- Calculation of $\boldsymbol{\lambda}(k)$, $k = 1, \dots, K$, via backward integration of (29) with final condition (31)
- Calculation of the reduced gradient (sometimes denoted $\mathbf{g}(k)$ below) from

$$\mathbf{g}(k) = \bar{J}_{\mathbf{u}(k)} = H_{\mathbf{u}(k)} = \Phi_{\mathbf{u}(k)} + \mathbf{f}_{\mathbf{u}(k)}^T \boldsymbol{\lambda}(k+1) \quad (32)$$

Thus, if a control trajectory is changed by $\delta\mathbf{u}(k)$, a linear approximation of the corresponding change of the cost function is provided by

$$\delta J = \delta\bar{J} = \sum_{k=0}^{K-1} H_{\mathbf{u}(k)}^T \delta\mathbf{u}(k). \quad (33)$$

If the reduced gradient vanishes, i.e. $\bar{J}_{\mathbf{u}(k)} = \mathbf{0}$ for all $k \in [0, K-1]$, then all necessary conditions of optimality are satisfied, as may be immediately verified.

2.4.2 Basic Algorithmic Structure

The feasible direction algorithm for the discrete-time optimal control problems is based on a corresponding iterative algorithm for static optimization problems, see [Papageorgiou et al. \(1991\)](#), [Fletcher \(2013\)](#). The algorithm attempts calculation of a local minimum of $\bar{J}(\mathbf{u}(k))$ in the mK -dimensional space of the control variables $\mathbf{U}^T = [\mathbf{u}(0)^T \dots \mathbf{u}(K-1)^T]$. The algorithm starts with an initial guess trajectory $\mathbf{u}^{(0)}(k)$ (upper indices in parenthesis indicate iteration number). At each iteration l , the algorithm modifies the current iterate $\mathbf{u}^{(l)}(k)$ so as to decrease the value of the cost function. The equality constraints (12), (13) are satisfied at each iteration. This section presents the basic algorithmic structure whilst subsequent sections provide more information on particular algorithmic steps.

The algorithmic steps are as follows:

- a) Guess an initial trajectory $\mathbf{u}^{(0)}(k), 0 \leq k \leq K-1$; calculate $\mathbf{x}^{(0)}(k)$ from (12), (13) and $\boldsymbol{\lambda}^{(0)}(k)$ from (29), (31); calculate from (32) the reduced gradient $\mathbf{g}^{(0)}(k) = \mathbf{H}_{\mathbf{u}(k)}^{(0)}$; set the iteration index $l = 0$.
- b) Specify a **search direction** (descent direction) $\mathbf{s}^{(l)}(k), k = 0, \dots, K-1$.
- c) Specify a scalar step $\alpha^{(l)} > 0$ by solving the following one-dimensional minimisation problem (**Line Optimization**)

$$\min_{\alpha > 0} \bar{J}[\mathbf{u}^{(l)}(k) + \alpha \mathbf{s}^{(l)}(k)]. \quad (34)$$

Set

$$\mathbf{u}^{(l+1)}(k) = \mathbf{u}^{(l)}(k) + \alpha^{(l)} \mathbf{s}^{(l)}(k), \quad k \in [0, K-1] \quad (35)$$

and calculate the corresponding $\mathbf{x}^{(l+1)}(k)$ from (12), $\boldsymbol{\lambda}^{(l+1)}(k)$ from (29) and $\mathbf{g}^{(l+1)}(k)$ from (32).

- d) If a convergence test is satisfied, stop.
- e) Start a new iteration $l := l + 1$; go to (b).

At each iteration, a descent direction is specified first, within step (b). Step (c) specifies a line minimum on the search direction which becomes the new iterate for the next iteration.

The algorithm may be shown to converge under mild assumptions to a local minimum.

The computation time has been empirically observed to increase roughly proportionally with the problem dimension.

In order to guarantee a reduction of the cost function at each iteration, the search direction in (b) must always be a **descent direction**. This means that for a small change $\delta \mathbf{u}^{(l)}(k) = \alpha \mathbf{s}^{(l)}(k)$, $\alpha > 0$, we must have according to (33)

$$\delta J^{(l)} = \sum_{k=0}^{K-1} H_{\mathbf{u}^{(k)}}^{(l)T} \delta \mathbf{u}^{(l)}(k) < 0. \quad (36)$$

With the general notation

$$(\chi, \psi) = \sum_{k=0}^{K-1} \chi(k)^T \psi(k) \quad (37)$$

we may express the descent condition (36) by

$$(\mathbf{s}^{(l)}, \mathbf{g}^{(l)}) < 0. \quad (38)$$

2.4.3 Specification of a Search Direction

Steepest Descent

The simplest but unfortunately the least efficient method of specification of a search direction is **steepest descent**

$$\mathbf{s}^{(l)}(k) = -\mathbf{g}^l(k), \quad k \in [0, K - 1] \quad (39)$$

that obviously satisfies the descent condition (38), unless $\mathbf{g}^l(k) = \mathbf{0} \quad \forall k \in [0, K - 1]$, in which case a local minimum has been found. Steepest descent typically leads to a quick approach of the minimum, if the initial guess $\mathbf{u}^{(0)}(k)$ was chosen far from the minimum. However, in a vicinity of the minimum the method is known to be not very efficient.

Quasi-Newton Methods

Quasi-Newton methods require more complex calculations for the specification of a search direction but are typically far more efficient than steepest descent. There are two main Quasi-Newton methods, namely **DFP** and **BFGS**.

The search direction calculation according to DFP is as follows

$$\mathbf{s}^{(0)}(k) = -\mathbf{g}^{(0)}(k), \quad k \in [0, K - 1] \quad (40)$$

and for $l > 0$ (omitting the time index k for convenience; each of the formulas below to be executed for all $k \in [0, K - 1]$)

$$\boldsymbol{\delta}^{(l-1)} = \mathbf{u}^{(l)} - \mathbf{u}^{(l-1)} \quad (41)$$

$$\mathbf{y}^{(l-1)} = \mathbf{g}^{(l)} - \mathbf{g}^{(l-1)} \quad (42)$$

$$\mathbf{z}^{(l-1)} = \mathbf{y}^{(l-1)} + \sum_{j=0}^{l-2} [(\mathbf{v}^{(j)}, \mathbf{y}^{(l-1)})\mathbf{v}^{(j)} - (\mathbf{w}^{(j)}, \mathbf{y}^{(l-1)})\mathbf{w}^{(j)}] \quad (43)$$

$$\mathbf{v}^{(l-1)} = (\boldsymbol{\delta}^{(l-1)}, \mathbf{y}^{(l-1)})^{-1/2} \boldsymbol{\delta}^{(l-1)} \quad (44)$$

$$\mathbf{w}^{(l-1)} = (\mathbf{z}^{(l-1)}, \mathbf{y}^{(l-1)})^{-1/2} \mathbf{z}^{(l-1)} \quad (45)$$

$$\mathbf{s}^{(l)} = -\mathbf{g}^{(l)} - \sum_{j=0}^{l-1} [(\mathbf{v}^{(j)}, \mathbf{g}^{(l)})\mathbf{v}^{(j)} - (\mathbf{w}^{(j)}, \mathbf{g}^{(l)})\mathbf{w}^{(j)}]. \quad (46)$$

Because of the sums in (43), (46), the vectors $\mathbf{v}^{(j)}(k), \mathbf{w}^{(j)}(k)$ for **all** previous iterations $j = 0, \dots, l-1$ must be stored. This means that the storage requirements of the method increase steadily during application. This increase may be limited however through periodic restart.

The BFGS method also starts with (40). For $l \geq 1$ and for $\boldsymbol{\delta}^{(l-1)}, \mathbf{y}^{(l-1)}, \mathbf{v}^{(l-1)}, \mathbf{w}^{(l-1)}$ as in (41), (42), (44), (45) the specification of a search direction follows the following formulas

$$\mathbf{z}^{(l-1)} = \mathbf{y}^{(l-1)} + \sum_{j=0}^{l-2} [(\mathbf{v}^{(j)}, \mathbf{y}^{(l-1)})\mathbf{v}^{(j)} - (\mathbf{w}^{(j)}, \mathbf{y}^{(l-1)})\mathbf{w}^{(j)} + (\mathbf{b}^{(j)}, \mathbf{y}^{(l-1)})\mathbf{b}^{(j)}] \quad (47)$$

$$\mathbf{b}^{(l-1)} = (\boldsymbol{\delta}^{(l-1)}, \mathbf{y}^{(l-1)})^{-1/2} (\mathbf{y}^{(l-1)}, \mathbf{z}^{(l-1)})^{1/2} \mathbf{v}^{(l-1)} - \mathbf{w}^{(l-1)} \quad (48)$$

$$\mathbf{s}^{(l)} = -\mathbf{g}^{(l)} - \sum_{j=0}^{l-1} [(\mathbf{v}^{(j)}, \mathbf{g}^{(l)})\mathbf{v}^{(j)} - (\mathbf{w}^{(j)}, \mathbf{g}^{(l)})\mathbf{w}^{(j)} + (\mathbf{b}^{(j)}, \mathbf{g}^{(l)})\mathbf{b}^{(j)}]. \quad (49)$$

These formulas indicate that the computational effort per iteration for BFGS is higher than for DFP. Moreover BFGS requires storage of three vectors $\mathbf{v}^{(j)}(k), \mathbf{w}^{(j)}(k), \mathbf{b}^{(j)}(k)$ from all previous iterations $j = 1, \dots, l - 1$.

Both BFGS and DFP may be shown to produce descent directions of search. For exact line search, BFGS and DFP produce identical results, but for inexact line search they may show different efficiency. All Quasi-Newton methods may be shown to terminate in at most mK iterations for quadratic cost functions and exact line search (Fletcher, 2013).

Conjugate Gradient Methods

Conjugate gradient methods approximate the simplicity of steepest descent and the efficiency of Quasi-Newton methods. There are two main conjugate gradient methods, namely **Fletcher-Reeves (FR)** and **Polak-Ribiere (PR)**.

The FR method starts with (40) and continues, for $l \geq 1$, with

$$\mathbf{s}^{(l)}(k) = -\mathbf{g}^{(l)}(k) + \beta^{(l)}\mathbf{s}^{(l-1)}(k), \quad k \in [0, K - 1] \quad (50)$$

with

$$\beta^{(l)} = \frac{(\mathbf{g}^{(l)}, \mathbf{g}^{(l)})}{(\mathbf{g}^{(l-1)}, \mathbf{g}^{(l-1)})} \quad (51)$$

The PR method starts with (40) and continues for $l \geq 1$ with (50) where $\beta^{(l)}$ is provided by

$$\beta^{(l)} = \frac{((\mathbf{g}^{(l)} - \mathbf{g}^{(l-1)}), \mathbf{g}^{(l)})}{(\mathbf{g}^{(l-1)}, \mathbf{g}^{(l-1)})} \quad (52)$$

Both FR and PR produce descent directions if the line search is exact, as can be easily shown. All conjugate gradient methods may be shown to terminate in mK iterations for quadratic cost functions and exact line search (Fletcher, 2013).

RPROP (Resilient backPROPagation) Method

RPROP does not require the line-search routine used in the algorithm described in section 3.2, since it calculates the necessary changes of the control variables at each iteration based only on the sign of the gradient components $\mathbf{g}_i(k)$. When the RPROP method is used (slightly modified by Kotsialos and Papageorgiou (2004) as compared to its original form Riedmiller and Braun (1993)), steps b) and c) of the algorithm described in section 2.4.2 are replaced by the following calculation:

$$\mathbf{u}^{l+1}(k) = \mathbf{sat} \left(\mathbf{u}^{(l)}(k) + \Delta \mathbf{u}^{(l)}(k) \right) \quad (53)$$

where the control variable increments $\Delta \mathbf{u}^{(l)}(k)$ are calculated based on the sign of the gradient $\mathbf{g}_i^{(l)}(k)$ and the increment $\Delta_i^{(l-1)}(k)$ of the previous iteration, as shown in the

following equation

$$\Delta u_i^{(l)}(k) = \begin{cases} -\text{sign}(\mathbf{g}_i^{(l)}(k))\eta^+|\Delta u_i^{(l-1)}(k)| & \text{if } \mathbf{g}_i^{(l-1)}(k)\mathbf{g}_i^{(l)}(k) > 0 \\ -\text{sign}(\mathbf{g}_i^{(l)}(k))\eta^-|\Delta u_i^{(l-1)}(k)| & \text{else} \end{cases} \quad (54)$$

where $0 < \eta^- < 1 < \eta^+$. Thus, if no change of the sign of $\mathbf{g}_i(k)$ between iterations $(l-1)$ and (l) , the corresponding increment $\Delta u_i^{(l)}(k)$ is increased as compared to $\Delta u_i^{(l-1)}(k)$ by a factor η^+ (typically $\eta^+ = 1.2$). If a sign change of $\mathbf{g}_i(k)$ occurred, then the algorithm has stepped over a minimum in the corresponding direction, hence, the new increment $\Delta u_i^{(l)}(k)$ is opposite in sign and reduced in size (typically $\eta^- = 0.5$) as compared to $\Delta u_i^{(l-1)}(k)$. The algorithm starts with $\Delta u_i^{(0)}(k) = \Delta_i$; the calculated $\Delta u_i^{(l)}(k)$ at each iteration may be restricted to lie in a prespecified interval $[\Delta_{\min}, \Delta_{\max}]$.

The RPROP method preserves feasibility of the overall algorithm but cannot guarantee a decrease of the objective function value at each iteration.

A Robust Convergent backProp (ARCprop) Method

As noted above, RPROP cannot cope with interactions between dimensions, and can consequently fail to converge. This section proposes a variant of RPROP that backtracks along all dimensions if a particular step does not achieve a sufficient decrease in error, and offers a proof of convergence of the new algorithm.

The basic idea of the algorithm proposed by [Bailey \(2015\)](#) is to take a series of downhill steps from the initial set of weights, until a vanishing error gradient indicates arrival at a local minimum. The algorithm terminates an iteration t if all $|\mathbf{g}_i^{(t)}| \leq \delta \ll 1$. If this vanishing gradient condition is not met, then a step of size $\Delta_i^{(t)}$ is made in the direction of descent along each dimension i . If the step results in a sufficient decrease in global error, then the search continues from that new, improved location, according to

$$\Delta_i^{(t)} := \begin{cases} \eta^+ \Delta_i^{(t-1)} & \text{if } \mathbf{g}_i^{(t)} \mathbf{g}_i^{(t-1)} > 0 \\ \eta^- \Delta_i^{(t-1)} & \text{if } \mathbf{g}_i^{(t)} \mathbf{g}_i^{(t-1)} < 0 \\ \Delta_i^{(t-1)} & \text{otherwise} \end{cases} \quad (55)$$

A sufficient decrease is taken to be greater than the target gradient threshold, δ , multiplied by the shortest component step length, $\min_i \Delta_i^{(t)}$. If the error does not go down by at

least that much, then the mean value theorem implies that some intermediate point must have a gradient small enough to satisfy the vanishing gradient criterion. In that case, a shorter step is initiated from the previous location; this assures convergence, as it prevents the algorithm from pursuing either increases in error or vanishingly small improvements in error, which could continue indefinitely.

The ARCprop algorithm is described by the following pseudo-code:

```

if  $\max_i |g_i^{(t)}| \leq \delta$  then return  $w^{(t)}$ 
if  $E^{(t)} > E^{(t-1)} - \delta \min_i \Delta_i^{(t-1)}$  then
    if  $\max_i \Delta_i^{t-1} \leq \Delta_{\min}$  then return  $w^{(t-1)}$ 
    for each  $w_i^{(t)}$  do
         $w_i^{(t)} := w_i^{(t-1)}; g_i^{(t)} = g_i^{(t-1)}$ 
         $\Delta_i^{(t)} := \max\{\eta^- \Delta_i^{t-1}, \Delta_{\min}\}$ 
    else
        for each  $w_i^{(t)}$  do
            
$$\Delta u_i^{(t)} = \begin{cases} \min\{\eta^+ \Delta_i^{(t-1)}, \Delta_{\max}\} & \text{if } g_i^{(t)} g_i^{(t-1)} > 0 \\ \max\{\eta^- \Delta_i^{(t-1)}, \Delta_{\min}\} & \text{if } g_i^{(t)} g_i^{(t-1)} < 0 \\ \Delta_i^{(t-1)} & \text{otherwise} \end{cases}$$

        for each  $w_i^{(t)}$  do
             $w_i^{(t+1)} := w_i^{(t)} - \Delta_i^{(t)} \text{sign}(g_i^{(t)})$ 

```

2.4.4 Constant Control Bounds

The concept of the reduced gradient may be readily extended to cover the case of simple but technically important inequality constraints of the form

$$\mathbf{u}_{\min}(k) \leq \mathbf{u}(k) \leq \mathbf{u}_{\max}(k), \quad 0 \leq k \leq K - 1 \quad (56)$$

where $\mathbf{u}_{\min}(k)$, $\mathbf{u}_{\max}(k)$ with $\mathbf{u}_{\min}(k) \leq \mathbf{u}_{\max}(k)$, are known lower and upper bounds respectively. In this case the reduced gradient γ with respect to both the state equations

and the active constraints has the components

$$\gamma_i(k) = \begin{cases} 0 & \text{if } u_i(k) = u_{\min,i}(k) \text{ and } s_i(k) < 0 \\ 0 & \text{if } u_i(k) = u_{\max,i}(k) \text{ and } s_i(k) > 0 \\ \mathbf{g}_i(k) & \text{else.} \end{cases} \quad (57)$$

Equation (57) implies that activation of a control constraint fixes the value of the corresponding control variable if the search direction tends to exceed the feasible control region. Thus, control variables that satisfy the first two cases of (57), have no contribution to the change of the cost function along the direction $\mathbf{s}(k)$, and as a consequence the corresponding component of the reduced gradient is zero. Equation (57) may also be interpreted as a projection of $\mathbf{g}(k)$ on the active inequality constraints, and for this reason the vector $\boldsymbol{\gamma}(k)$ is sometimes called the projected gradient.

Suitable modifications are applied to the algorithm of section 2.4.2 so that:

- the constraints (56) are always satisfied during the iterations
- the line search operates taking into account only the control variables that are not fixed at their upper or lower bounds.

2.5 ARRB Fuel Consumption Model

A family of four models for fuel consumption and emissions modeling was proposed by Bowyer et al. (1985). This family provides specific models to cover a wide range of traffic circumstances, from the performance of an individual vehicle driven in traffic to a model for a total door-to-door trip. The Biggs-Akcelik models are:

- an *instantaneous model*, that indicates the rate of fuel usage or pollutant emission of an individual vehicle continuously over time,
- an *elemental model*, that relates fuel usage or pollutant emission to traffic variables such as deceleration, acceleration, idling and cruising, etc. over a short road distance (e.g. the approach to an intersection),
- a *running speed model*, that gives emissions or fuel consumption for vehicles traveling

over an extended length of road (e.g. representing a network link) and

- an *average speed model*, that indicates level of emissions or fuel consumption over an entire journey.

The Australian Road Research Board (ARRB) instantaneous model (Energy-Related Model) (Biggs and Akcelik, 1984; Biggs and Akçelik, 1985; Biggs and Akcelik, 1986; Bowyer et al., 1985) is the basic (and most detailed) model. The other models are aggregations of this model, and require less and less information but are also increasingly less accurate. The elemental model is the next most detailed model, and is suitable for intersection or road section analysis where the focus is on an entity in the road system (such as the intersection or a traffic control device) rather than the individual vehicles negotiating that entity. The running speed model is suitable for application in strategic networks, for it can be used at the network link level. Regional 'sketch' planning studies which do not include formal (link-node) description of the transport network can make good use of the average speed model.

The Energy-Related Model For Estimating Car Fuel Consumption

The Energy-Related fuel consumption model described below estimates instantaneous values of fuel consumption from second-by-second speed and grade information. The model is an extended and modified version of the power model described by Post et al. (1984) and it is described in detail in Akçelik and Biggs (1987) and Bowyer et al. (1985). Basically, the model relates fuel consumption during a small increment, dt , to:

- (a) the fuel to maintain engine operation,
- (b) the energy consumed (work done) by the vehicle engine while traveling an increment of distance, dx , during this time period, and
- (c) the product of energy and acceleration during periods of positive acceleration.

Part (c) allows for the inefficient use of fuel during periods of high acceleration. Since energy is $dE = R_T dx$ where R_T is the total tractive force required to drive the vehicle along distance dx , the fuel consumed in the time increment, dt , is expressed as

$$dF = \begin{cases} \alpha dt + \beta_1 R_T dx + (\beta_2 a R_I dx)_{a>0} & \text{for } R_T > 0 \\ \alpha dt & \text{for } R_T \leq 0 \end{cases} \quad (58)$$

where

dF = increment of fuel consumed (ml) during travel along distance dx (m) and in time dt (s),

α = constant idle fuel rate (ml/s), which applies during all modes of driving as an estimate of fuel used to maintain engine operation),

β_1 = an efficiency parameter which relates fuel consumed to the energy provided by the engine, i.e. fuel consumption per unit of energy (ml/kJ),

β_2 = an efficiency parameter which relates fuel consumed during positive acceleration to the product of inertia energy and acceleration, i.e. fuel consumption per unit of energy-acceleration (ml/(kJ · m/s²)),

a = instantaneous acceleration (dv/dt) in m/s², which has a negative value for slowing down, and

R_T = total "tractive" force required to drive the vehicle, which is the sum of drag force (R_D), inertia force (R_I) and grade force (R_G) in kN (kilonewtons):

$$R_T = R_D + R_I + R_G \quad (59)$$

The resistive forces can be expressed as:

$$R_D = b_1 + b_2 v^2 \quad (60)$$

$$R_I = Ma/1000 \quad (61)$$

$$R_G = 9.81M(G/100)/1000 \quad (62)$$

where

v = speed (dx/dt) in m/s,

G = percent grade which has a negative value for downhill grade,

M = vehicle mass in kg, including occupants and any other load, and

b_1, b_2 = the vehicle parameters related mainly to rolling resistance and aerodynamic drag, but each containing a component due to drag associated with the engine. The parameters of drag function (60) are derived using steady-speed fuel consumption data. However, if data collected during coast-down in neutral are also available, a three-term function $R_D = b_1 + b_2v + b_3v^2$ can be derived where b_1, b_2 and b_3 are related to rolling, engine and aerodynamic drag, respectively.

The following parameter values derived for the Melbourne University test car (4.1-L Ford Cortina station-wagon with automatic transmission (Biggs and Akcelik, 1986)) were used for the analyses reported in this work:

$$M = 1680 \text{ kg}$$

$$\alpha = 0.666 \text{ ml/s}$$

$$\beta_1 = 0.0717 \text{ ml/kJ}$$

$$\beta_2 = 0.0344 \text{ ml/(kJ} \cdot \text{m/s}^2)$$

$$b_1 = 0.527 \text{ kN}$$

$$b_2 = 0.000948 \text{ kN(m/s)}^2$$

When the engine drag was allowed for separately, the three drag parameters found to be $b_1 = 0.269$, $b_2 = 0.0171$ and $b_3 = 0.000672$.

Fuel consumption per unit time (ml/s) can be expressed as:

$$f_t(v, a) = dF/dt = \begin{cases} \alpha + \beta_1 R_T v + \left(\frac{\beta_2 M a^2 v}{1000} \right)_{a>0} & \text{for } R_T > 0 \\ \alpha & \text{for } R_T \leq 0 \end{cases} \quad (63)$$

where the total tractive force required is:

$$R_T = b_1 + b_2v + b_3v^2 + \frac{Ma}{1000} + 9.81 \times 10^{-5} MG.$$

2.6 Smoothing Function

The ARRB fuel consumption model, presented in the previous section, is a non-smooth function (see Figure 1 and Figure 2), which means that it is a continuous function with a discontinuous first order derivative. A non-smooth model does not allow us to use available efficient gradient-based optimisation methods. Hence, it would be useful to have a nonlinear smooth model, expressed by means of functions that are differentiable everywhere in their domain.

Maximum Function

We look for the smooth form of the following function in general

$$x_{\max} \rightarrow \max\{x_1, \dots, x_n\} \quad (64)$$

Our smoothing approach is based on the method proposed in [Chen and Mangasarian \(1995\)](#), where the following smooth form of the plus function, i.e., $x^+ = \max\{0, x\}$, is proposed:

$$x^+ = \max\{0, x\} \approx x + \frac{1}{\alpha_s} \log(1 + e^{-\alpha_s x}) \quad \text{for } \alpha_s \gg 1 \quad (65)$$

and it is easily verified in [Jamshidnejad et al. \(2015\)](#) that for $\alpha_s \gg 1$ we have in general:

$$\max_{i=1, \dots, n} \{x_i\} \approx \frac{1}{\alpha_s} \log \sum_{i=1}^n e^{\alpha_s x_i} \quad (66)$$

with α_s a smoothing parameter.

So the ARRB fuel consumption model is transformed as we can see below

$$f(v, a) = \begin{cases} \frac{1}{\alpha_s} (\log(e^{\alpha_s \alpha} + e^{\alpha_s \beta_1 R_T v + \frac{\beta_2 M a^2 v}{1000}})) & \text{for } a > 0 \\ \frac{1}{\alpha_s} (\log(e^{\alpha_s \alpha} + e^{\alpha_s \beta_1 R_T v})) & \text{for } a \leq 0 \end{cases} \quad (67)$$

assuming that each x_i of (66) is expressed as follows:

$$x_1 = \alpha \quad (68)$$

$$x_2 = \begin{cases} \beta_1 R_T v + \frac{\beta_2 M a^2 v}{1000} & \text{for } a > 0 \\ \beta_1 R_T v & \text{for } a \leq 0 \end{cases} \quad (69)$$

For the choice of the parameter α_s , we have tested different values in order to see the behavior of the smoothed model. As expected, and can be verified from figure 2, the smaller the value of the parameter α_s is (see the case where $\alpha_s = 1$), the more the smoothed model diverge from the original model, while as the value is increased it tends to approach the fuel consumption model. From the values tested the more appropriate choice of α_s was this of the value 20, as it approaches the fuel consumption model quite satisfactory. For lower values than the selected α_s , as we already mentioned, the results were not acceptable as the difference of the fuel consumption values was sensible and for greater values, the difference between the results was insignificant or even the resulted smoothed model had the same behavior as the original one.

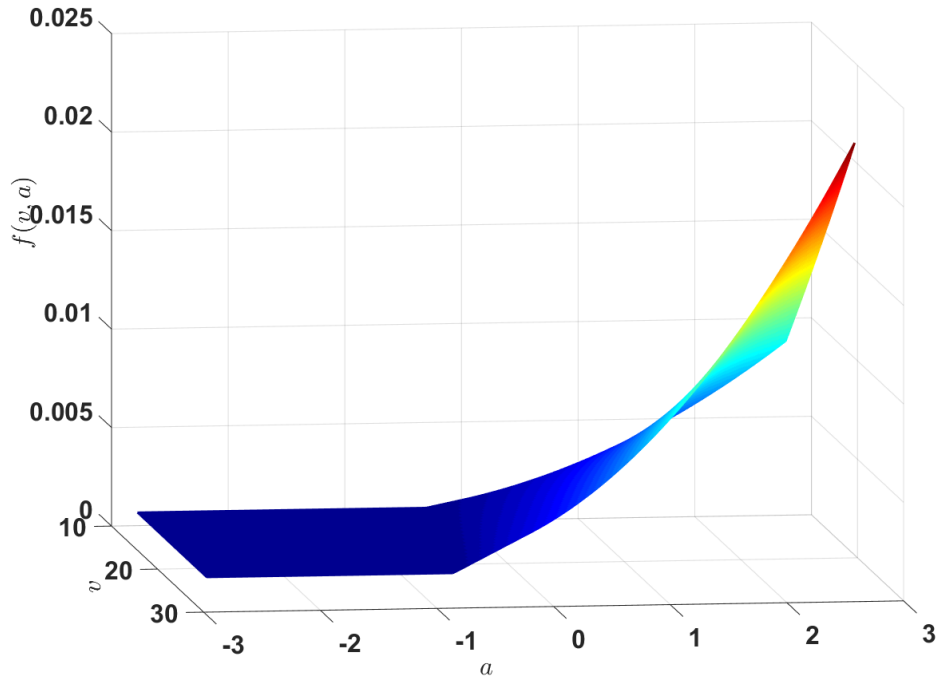


Figure 1: A 3D representation of ARRB Fuel Consumption Model, instantaneous fuel consumption

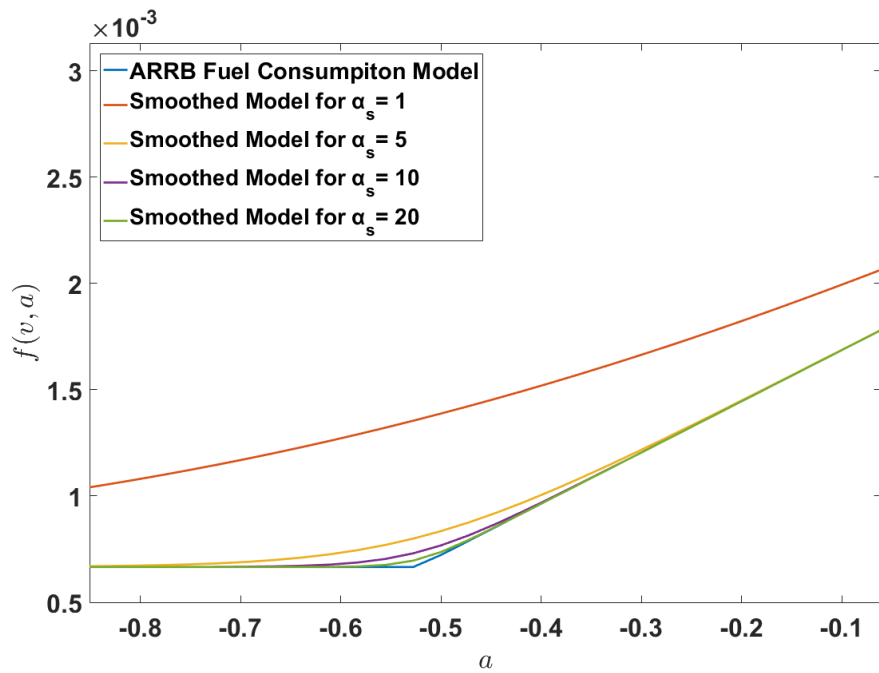


Figure 2: A 2D representation (assuming that the value of speed is constant, $v = 15$ m/s) of ARRB Fuel Consumption Model, instantaneous fuel consumption and the smoothed model for different values of α_s

3

Description of the problem

We consider a single lane freeway and a single lane on-ramp, which leads to an acceleration lane, as shown in Figure 3. We define a merge point (entrance to the highway) at the end of the acceleration lane where vehicles will merge with the main flow of the highway.

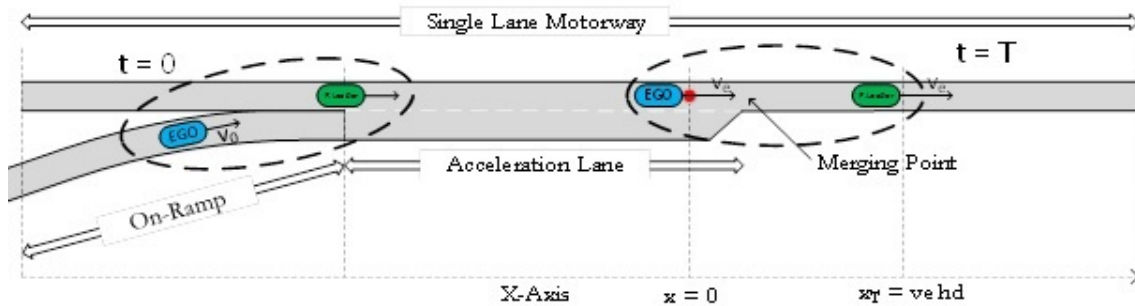


Figure 3: The positions of the "EGO" vehicle and its putative leader at the beginning and the end of the merging procedure.¹

The scenario chosen for the study, is the case where a vehicle coming from the on-ramp appropriately adjusts its speed and enters the freeway. The vehicle whose motion is studied, is called "EGO", while the leader vehicle (green in Figure 3) is called "Leader".

The initial conditions of our scenario is that the vehicle "EGO" is starting from a given initial position x_0 and should reach the end position at $x = 0$, as shown in Figure 3, at time T . Also, we consider that it has an initial velocity v_0 and aims a final velocity v_e at time T . This final speed of the vehicle is equal to the (given) speed of the leading ("Leader") vehicle. The leading vehicle is considered to perform linear uniform motion at a constant speed, without this affecting our methodology, as the solution that will emerge depends only on final velocity v_e which is considered to be known and available for the "EGO" vehicle. In fact, the knowledge of this final velocity is a complex problem that

¹(Ntousakis et al., 2016)

requires specialized technological means (sensors, communications, etc.) and specialized forecasting techniques in order the speed to be correctly predicted. The total time T is defined as the sum of the time required in order the vehicle in front to reach the final position ($x = 0$) plus the time of the distance of the leading's vehicle front bumper from the front bumper of the following vehicle (headway time).

For the needs of this thesis we will assume 5 scenarios to be tested, as we can see below. The first scenario is the case where we have at the beginning negative and then positive but continuously increasing acceleration case. Scenario 2 is a positive increasing acceleration case, while scenario 3 is a positive and then negative decreasing acceleration case. Scenario 4 and 5 are increasing and decreasing negative acceleration cases, respectively. In the first scenario, the initial speed of the "EGO" vehicle will be $v_0 = 54$ km/h, the final speed $v_e = 72$ km/h and the distance to be covered is 0.30 km; in the second scenario the initial and final speed are also $v_0 = 54$ km/h and $v_e = 72$ km/h, respectively, and the distance that the vehicle has to cover is 0.32 km; in the third scenario, the initial and final speed are $v_0 = 54$ km/h and $v_e = 90$ km/h and the distance is 0.37 km; and as far as the fourth and fifth scenarios are concerned, the initial speed is $v_0 = 72$ km/h, the final speed $v_e = 54$ km/h and the distances are 0.42 km and 0.44 km, respectively.

Scenario 1: $v_0 = 54$ km/h, $v_e = 72$ km/h, $x_e = 0.30$ km.

Scenario 2: $v_0 = 54$ km/h, $v_e = 72$ km/h, $x_e = 0.32$ km.

Scenario 3: $v_0 = 54$ km/h, $v_e = 90$ km/h, $x_e = 0.37$ km.

Scenario 4: $v_0 = 72$ km/h, $v_e = 54$ km/h, $x_e = 0.42$ km.

Scenario 5: $v_0 = 72$ km/h, $v_e = 54$ km/h, $x_e = 0.44$ km.

3.1 Taylor Approximation of the Fuel Consumption Model

We apply a quadratic approximation around a point $(v = v_k, a = a_k)$ (Taylor expansion) in a general fuel consumption function $f(v, a)$

$$q(v, a) = f(v_k, a_k) + \nabla f(v_k, a_k)^t (v - v_k, a - a_k) + 1/2 \begin{pmatrix} v - v_k \\ a - a_k \end{pmatrix} \nabla^2 f(v_k, a_k) \begin{pmatrix} v - v_k \\ a - a_k \end{pmatrix} \quad (70)$$

where v denotes the velocity, a the acceleration, $\nabla f(v_k, a_k)$ the gradient and $\nabla^2 f(v_k, a_k)$ the Hessian of f at $(v = v_k, a = a_k)$.

If we define

$$\nabla f(v_k, a_k) = \begin{pmatrix} g_1 & g_2 \end{pmatrix}^t \quad (71)$$

$$\nabla^2 f(v_k, a_k) = \begin{pmatrix} h_{11} & h_{12} \\ h_{21} & h_{22} \end{pmatrix} \quad (72)$$

then the approximation function becomes

$$\begin{aligned} q(v, a) = & \frac{a^2 h_{22}}{2} + \frac{v^2 h_{11}}{2} + v \left(g_1 + \frac{1}{2} a (h_{12} + h_{21}) - \frac{1}{2} a_k (h_{12} + h_{21}) - h_{11} v_k \right) \\ & + a \left(g_2 - a_k h_{22} - \frac{1}{2} (h_{12} + h_{21}) v_k \right) \\ & + \frac{1}{2} \left(2f(v_k, a_k) - 2a_k g_2 + a_k^2 h_{22} + a_k (h_{12} + h_{21}) v_k + v_k (-2g_1 + h_{11} v_k) \right) \end{aligned} \quad (73)$$

3.2 Optimal Control Methodology

Based on the above description of the problem, we proceed to the mathematical modeling of the problem presented in Chapter 2. The system is described by the following state variables:

$$\dot{x} = v \quad (74)$$

$$\dot{v} = a \quad (75)$$

where x is the position, v is the velocity and a is the acceleration (control variable - u).

The objective is to bring the system from the initial condition $\mathbf{x}_0 = [x_0, v_0]^T$ to the final condition $\mathbf{x}_e = [x_e, v_e]^T$ by time T , by minimizing the criterion

$$J = \int_0^T q(v, a) dt \quad (76)$$

where, the function $q(v, a)$ is the Taylor approximation of the ARRB fuel consumption model which we described in section 2.5.

In order to find the solution of the optimal control problem, we first write its Hamiltonian equation, based on (5)

$$H(v, a) = q(v, a) + \lambda_1 v + \lambda_2 a \quad (77)$$

where λ_1 and λ_2 are the costate variables.

Therefore substituting (73) into (77) we have

$$\begin{aligned} H(v, a) = & \frac{a^2 h_{22}}{2} + \frac{v^2 h_{11}}{2} \\ & + \frac{1}{2} \left(2f_k - 2a_k g_2 + a_k^2 h_{22} + a_k (h_{12} + h_{21}) v_k + v_k (-2g_1 + h_{11} v_k) \right) \\ & + v \left(g_1 + \frac{1}{2} a (h_{12} + h_{21}) - \frac{1}{2} a_k (h_{12} + h_{21}) - h_{11} v_k + \lambda_1 \right) \\ & + a \left(g_2 - a_k h_{22} - \frac{1}{2} (h_{12} + h_{21}) v_k + \lambda_2 \right) \end{aligned} \quad (78)$$

In order to minimize H with respect to the vector variable a , we find the optimal control (8)

$$\begin{aligned} \frac{\partial H}{\partial a} = 0 \Rightarrow \\ \Rightarrow g_2 + \frac{1}{2} (2(a - a_k) h_{22} + h_{12} (v - v_k) + h_{21} (v - v_k)) + \lambda_2 = 0 \end{aligned} \quad (79)$$

and solving (79) for a , we have

$$a_0 = -\frac{(h_{12} + h_{21}) v}{2h_{22}} + \frac{-2g_2 + 2a_k h_{22} + (h_{12} + h_{21}) v_k}{2h_{22}} - \frac{\lambda_2}{h_{22}} \quad (80)$$

Then, we find the optimal function (9) substituting a_0 from (80) to (78)

$$\begin{aligned} H(v, a = a_0) = & f_k - \frac{g_2^2}{2h_{22}} + \left(\frac{h_{11}}{2} - \frac{h_{12}^2}{8h_{22}} - \frac{h_{12}h_{21}}{4h_{22}} - \frac{h_{21}^2}{8h_{22}} \right) v^2 \\ & - g_1 v_k + \frac{g_2 h_{22} v_k}{2h_{22}} + \frac{h_{11} v_k^2}{2} - \frac{h_{12}^2 v_k^2}{8h_{22}} - \frac{h_{12} h_{21} v_k^2}{4h_{22}} \\ & - \frac{h_{21}^2 v_k^2}{8h_{22}} + \left(a_k - \frac{g_2}{h_{22}} + \frac{h_{12} v_k}{2h_{22}} + \frac{h_{21} v_k}{2h_{22}} \right) \lambda_2 - \frac{\lambda_2^2}{2h_{22}} \\ & + v \left(g_1 - \frac{g_2 h_{12}}{2h_{22}} - \frac{g_2 h_{21}}{2h_{22}} - h_{11} v_k + \frac{h_{12}^2 v_k}{4h_{22}} + \frac{h_{12} h_{21} v_k}{2h_{22}} \right. \\ & \left. + \frac{h_{21}^2 v_k}{4h_{22}} + \lambda_1 + \left(-\frac{h_{12}}{2h_{22}} - \frac{h_{21}}{2h_{22}} \right) \lambda_2 \right) \end{aligned} \quad (81)$$

From (10) and (11), the necessary conditions for optimality are:

$$\dot{x} = \frac{\partial H_0}{\partial \lambda_1} = v \quad (82)$$

$$\dot{v} = \frac{\partial H_0}{\partial \lambda_2} = -\frac{(h_{12} + h_{21})v}{2h_{22}} + \frac{-2g_2 + 2a_k h_{22} + (h_{12} + h_{21})v_k}{2h_{22}} - \frac{\lambda_2}{h_{22}} \quad (83)$$

$$\dot{\lambda}_1 = -\frac{\partial H_0}{\partial x} = 0 \quad (84)$$

$$\begin{aligned} \dot{\lambda}_2 = -\frac{\partial H_0}{\partial v} = & \left(-h_{11} + \frac{(h_{12} + h_{21})^2}{4h_{22}} \right) v \\ & - \frac{-2g_2(h_{12} + h_{21}) + 4g_1 h_{22} + \left((h_{12} + h_{21})^2 - 4h_{11} h_{22} \right) v_k}{4h_{22}} \\ & - \lambda_1 + \frac{(h_{12} + h_{21})\lambda_2}{2h_{22}} \end{aligned} \quad (85)$$

In order to solve the ODE system (82)-(85), the initial and final conditions of the problem will be used: $x(0) = x_0$, $x(T) = 0$, $v(0) = v_0$ and $v(T) = v_e$. The resulting state and costate equations are described as follows

$$\begin{aligned} \lambda_1(t) = & (g_1(4\sqrt{h_{22}} + 2\sqrt{h_{11}}T - 2e^{\frac{\sqrt{h_{11}}T}{\sqrt{h_{22}}}}(2\sqrt{h_{22}} - \sqrt{h_{11}}T)) \\ & + a_k(h_{12} + h_{21})(-2\sqrt{h_{22}} - \sqrt{h_{11}}T + e^{\frac{\sqrt{h_{11}}T}{\sqrt{h_{22}}}}(2\sqrt{h_{22}} - \sqrt{h_{11}}T)) \\ & - 2h_{11}((-1 + e^{\frac{\sqrt{h_{11}}T}{\sqrt{h_{22}}}})\sqrt{h_{22}}(v_0 + v_e - 2v_k) + (1 + e^{\frac{\sqrt{h_{11}}T}{\sqrt{h_{22}}}}) \\ & \sqrt{h_{11}}(Tv_k + x_0))) \Bigg/ \left(4(-1 + e^{\frac{\sqrt{h_{11}}T}{\sqrt{h_{22}}}})\sqrt{h_{22}} - 2(1 + e^{\frac{\sqrt{h_{11}}T}{\sqrt{h_{22}}}})\sqrt{h_{11}}T \right) \end{aligned} \quad (86)$$

$$\begin{aligned}
\lambda_2(t) = & \left(e^{-\frac{\sqrt{h_{11}}t}{\sqrt{h_{22}}}} \left(-2e^{\frac{\sqrt{h_{11}}(t+T)}{\sqrt{h_{22}}}} \sqrt{h_{22}}(-4g_2 + 4a_k h_{22} - (h_{12} + h_{21})(v_0 + v_e - 2v_k)) \right. \right. \\
& - e^{\frac{2\sqrt{h_{11}}t}{\sqrt{h_{22}}}} (h_{12} + h_{21} + 2\sqrt{h_{11}}\sqrt{h_{22}})(\sqrt{h_{22}}(v_0 - v_e) + \sqrt{h_{11}}(Tv_0 + x_0)) \\
& - e^{\frac{2\sqrt{h_{11}}T}{\sqrt{h_{22}}}} (-h_{12} - h_{21} + 2\sqrt{h_{11}}\sqrt{h_{22}})(\sqrt{h_{22}}(-v_0 + v_e) + \sqrt{h_{11}}(Tv_0 + x_0)) \\
& + e^{\frac{\sqrt{h_{11}}(2t+T)}{\sqrt{h_{22}}}} (h_{12} + h_{21} + 2\sqrt{h_{11}}\sqrt{h_{22}})(\sqrt{h_{22}}(v_0 - v_e) + \sqrt{h_{11}}(Tv_e + x_0)) \\
& + e^{\frac{\sqrt{h_{11}}T}{\sqrt{h_{22}}}} (-h_{12} - h_{21} + 2\sqrt{h_{11}}\sqrt{h_{22}})(\sqrt{h_{22}}(-v_0 + v_e) + \sqrt{h_{11}}(Tv_e + x_0)) \\
& + e^{\frac{\sqrt{h_{11}}t}{\sqrt{h_{22}}}} (-2g_2(2\sqrt{h_{22}} + \sqrt{h_{11}}T) + 2a_k(2h_{22}^{\frac{3}{2}} + \sqrt{h_{11}}h_{22}T) - (h_{12} + h_{21}) \\
& (\sqrt{h_{22}}(v_0 + v_e - 2v_k) - \sqrt{h_{11}}(Tv_k + x_0))) \\
& + e^{\frac{\sqrt{h_{11}}(t+2T)}{\sqrt{h_{22}}}} (g_2(-4\sqrt{h_{22}} + 2\sqrt{h_{11}}T) + a_k(4h_{22}^{\frac{3}{2}} - 2\sqrt{h_{11}}h_{22}T) - (h_{12} + h_{21}) \\
& (\sqrt{h_{22}}(v_0 + v_e - 2v_k) + \sqrt{h_{11}}(Tv_k + x_0)))) \Big/ \\
& \left(2(-1 + e^{\frac{\sqrt{h_{11}}T}{\sqrt{h_{22}}}})(-2\sqrt{h_{22}} - \sqrt{h_{11}}T + e^{\frac{\sqrt{h_{11}}T}{\sqrt{h_{22}}}}(2\sqrt{h_{22}} - \sqrt{h_{11}}T)) \right)
\end{aligned} \tag{87}$$

$$\begin{aligned}
x(t) = & \left(e^{-\frac{\sqrt{h_{11}}t}{\sqrt{h_{22}}}} \left(2e^{\frac{\sqrt{h_{11}}(t+T)}{\sqrt{h_{22}}}} \sqrt{h_{11}}\sqrt{h_{22}}(-Tv_e + t(v_0 + v_e) + x_0) \right. \right. \\
& + e^{\frac{2\sqrt{h_{11}}T}{\sqrt{h_{22}}}} (h_{22}(v_0 - v_e) - \sqrt{h_{11}}\sqrt{h_{22}}(Tv_0 + x_0)) \\
& + e^{\frac{2\sqrt{h_{11}}t}{\sqrt{h_{22}}}} (h_{22}(-v_0 + v_e) - \sqrt{h_{11}}\sqrt{h_{22}}(Tv_0 + x_0)) \\
& + e^{\frac{\sqrt{h_{11}}(2t+T)}{\sqrt{h_{22}}}} (h_{22}(v_0 - v_e) + \sqrt{h_{11}}\sqrt{h_{22}}(Tv_e + x_0)) \\
& + e^{\frac{\sqrt{h_{11}}T}{\sqrt{h_{22}}}} (h_{22}(-v_0 + v_e) - \sqrt{h_{11}}\sqrt{h_{22}}(Tv_e + x_0)) \\
& + e^{\frac{\sqrt{h_{11}}t}{\sqrt{h_{22}}}} (h_{22}(v_0 - v_e) + h_{11}(t - T)x_0 - \sqrt{h_{11}}\sqrt{h_{22}}(-Tv_0 + t(v_0 + v_e) + x_0)) \\
& - e^{\frac{\sqrt{h_{11}}(t+2T)}{\sqrt{h_{22}}}} (h_{22}(v_0 - v_e) + h_{11}(t - T)x_0 + \sqrt{h_{11}}\sqrt{h_{22}}(-Tv_0 + t(v_0 + v_e) + x_0))) \Big/ \\
& \left((-1 + e^{\frac{\sqrt{h_{11}}T}{\sqrt{h_{22}}}}) \sqrt{h_{11}}(2\sqrt{h_{22}} + \sqrt{h_{11}}T + e^{\frac{\sqrt{h_{11}}T}{\sqrt{h_{22}}}}(-2\sqrt{h_{22}} + \sqrt{h_{11}}T)) \right)
\end{aligned} \tag{88}$$

$$\begin{aligned}
v(t) = & \left(e^{-\frac{\sqrt{h_{11}}t}{\sqrt{h_{22}}}} \left(-2e^{\frac{\sqrt{h_{11}}(t+T)}{\sqrt{h_{22}}}} \sqrt{h_{22}}(v_0 + v_e) + e^{\frac{\sqrt{h_{11}}t}{\sqrt{h_{22}}}} (\sqrt{h_{22}}(v_0 + v_e) - \sqrt{h_{11}}x_0) \right. \right. \\
& + e^{\frac{\sqrt{h_{11}}(t+2T)}{\sqrt{h_{22}}}} (\sqrt{h_{22}}(v_0 + v_e) - \sqrt{h_{11}}x_0) + e^{\frac{2\sqrt{h_{11}}T}{\sqrt{h_{22}}}} (\sqrt{h_{22}}(v_0 - v_e) \\
& - \sqrt{h_{11}}(Tv_0 + x_0)) + e^{\frac{2\sqrt{h_{11}}t}{\sqrt{h_{22}}}} (\sqrt{h_{22}}(v_0 - v_e) + \sqrt{h_{11}}(Tv_0 + x_0)) \\
& - e^{\frac{\sqrt{h_{11}}(2t+T)}{\sqrt{h_{22}}}} (\sqrt{h_{22}}(v_0 - v_e) + \sqrt{h_{11}}(Tv_e + x_0)) + e^{\frac{\sqrt{h_{11}}T}{\sqrt{h_{22}}}} (\sqrt{h_{22}}(-v_0 + v_e) + \\
& \left. \left. \sqrt{h_{11}}(Tv_e + x_0)) \right) \right) / \\
& \left((-1 + e^{\frac{\sqrt{h_{11}}T}{\sqrt{h_{22}}}}) (-2\sqrt{h_{22}} - \sqrt{h_{11}}T + e^{\frac{\sqrt{h_{11}}T}{\sqrt{h_{22}}}} (2\sqrt{h_{22}} - \sqrt{h_{11}}T)) \right)
\end{aligned} \tag{89}$$

Finally, in order to find the optimal acceleration function, we calculate the derivative of (89)

$$\begin{aligned}
a(t) = & \left(e^{-\frac{\sqrt{h_{11}}t}{\sqrt{h_{22}}}} \sqrt{h_{11}} \left(e^{2\frac{\sqrt{h_{11}}T}{\sqrt{h_{22}}}} (\sqrt{h_{22}}(v_0 + v_e) - \sqrt{h_{11}}(Tv_0 + x_0)) \right. \right. \\
& - e^{\frac{2\sqrt{h_{11}}t}{\sqrt{h_{22}}}} (\sqrt{h_{22}}(v_0 - v_e) + \sqrt{h_{11}}(Tv_0 + x_0)) \\
& + e^{\frac{\sqrt{h_{11}}(2t+T)}{\sqrt{h_{22}}}} (\sqrt{h_{22}}(v_0 - v_e) + \sqrt{h_{11}}(Tv_e + x_0)) \\
& \left. \left. + e^{\frac{\sqrt{h_{11}}T}{\sqrt{h_{22}}}} (\sqrt{h_{22}}(-v_0 + v_e) + \sqrt{h_{11}}(Tv_e + x_0)) \right) \right) / \\
& \left((-1 + e^{\frac{\sqrt{h_{11}}T}{\sqrt{h_{22}}}}) \sqrt{h_{22}} (2\sqrt{h_{22}} + \sqrt{h_{11}}T + e^{\frac{\sqrt{h_{11}}T}{\sqrt{h_{22}}}} (-2\sqrt{h_{22}} + \sqrt{h_{11}}T)) \right)
\end{aligned} \tag{90}$$

4

4.1 Analytic Solution of Taylor Approximation

Having the results of the optimal states and control of the Taylor approximation problem, we test the different scenarios described at the beginning of the chapter 3 in order to check how the fuel consumption rate varies.

In the following figures, we present the position, speed, acceleration and fuel consumption rate diagrams versus time. At the beginning we test Scenarios 1-3 where the initial speed of the "EGO" vehicle is smaller than the final speed and we change the distance that the vehicle has to cover as it is shown in Figure 4 - Figure 6. In Figure 7 and Figure 8 we check Scenarios 4-5 where the initial speed is greater than the final speed and the condition that changes is also the distance.

The results that we derived from all scenarios are according to our expectations. In Scenarios 1-3, where the final speed is greater than the initial speed the vehicle mostly accelerates in order to reach the desired speed and position and only decelerates so that it fulfills the terminal conditions. Also, Scenario 3 has the higher fuel consumption rate as it has the greater acceleration and has to cover more kilometers to reach its destination. In Scenario 3, we can notice as well that, during the last seconds, the fuel consumption rate is stable and equal to the idle consumption α . This happens because at the last seconds the total tractive force, R_T , is smaller than zero. On the other hand, in Scenarios 4-5 the vehicle decelerates as the final initial speed is greater than the final speed and both Scenarios have less fuel consumption than the Scenarios 1-3, and the fuel consumption rate is decreasing.

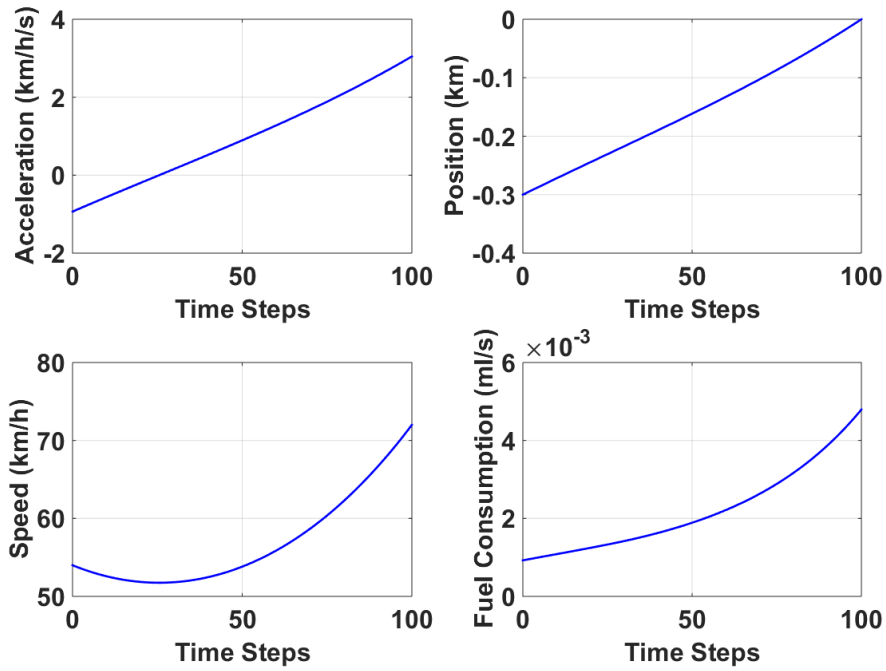


Figure 4: Graphical representation of the optimal solution, regarding the minimisation of the approximated fuel consumption model for scenario 1.

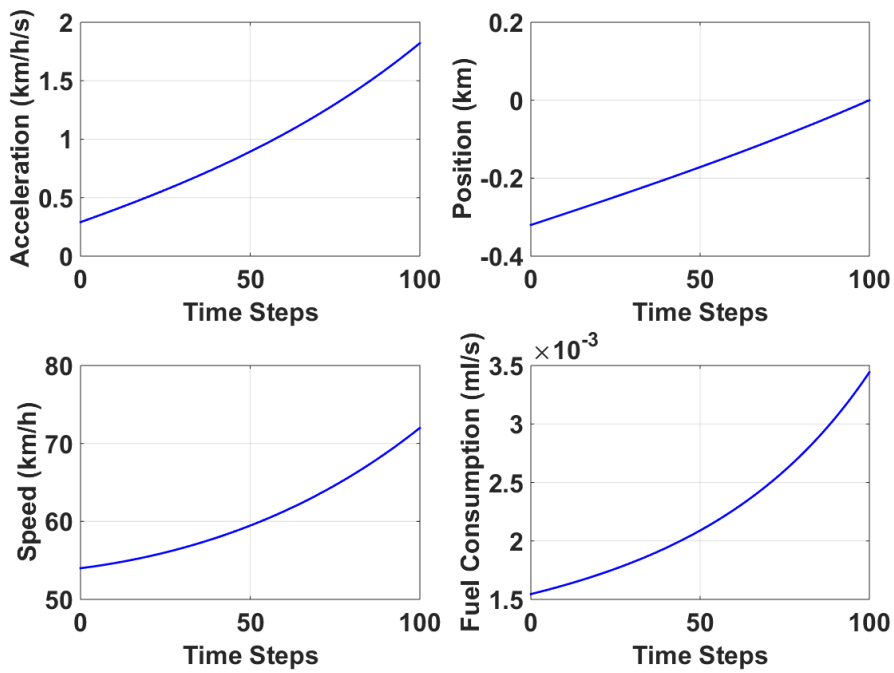


Figure 5: Graphical representation of the optimal solution, regarding the minimisation of the approximated fuel consumption model for scenario 2.

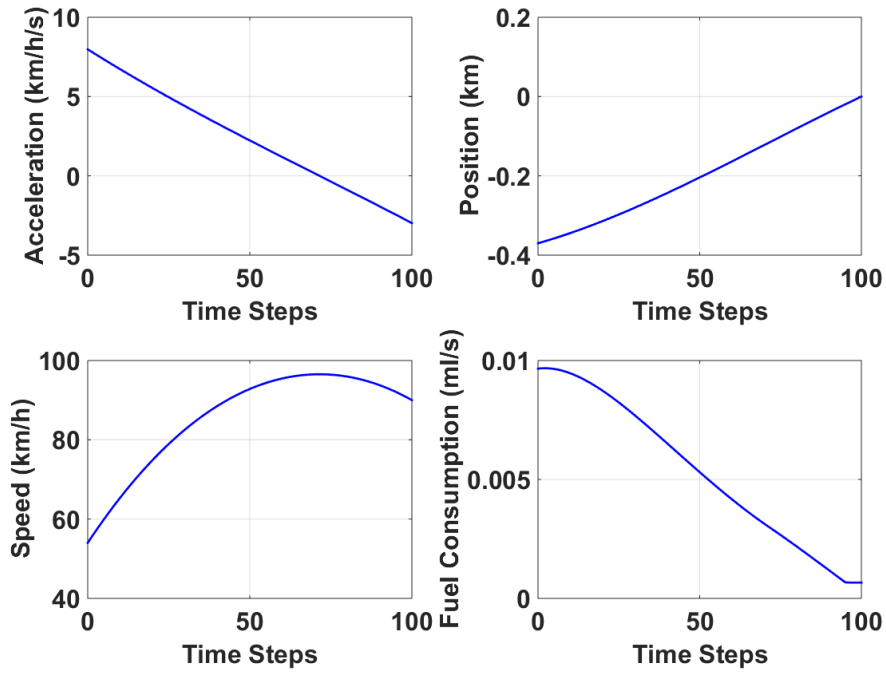


Figure 6: Graphical representation of the optimal solution, regarding the minimisation of the approximated fuel consumption model for scenario 3.

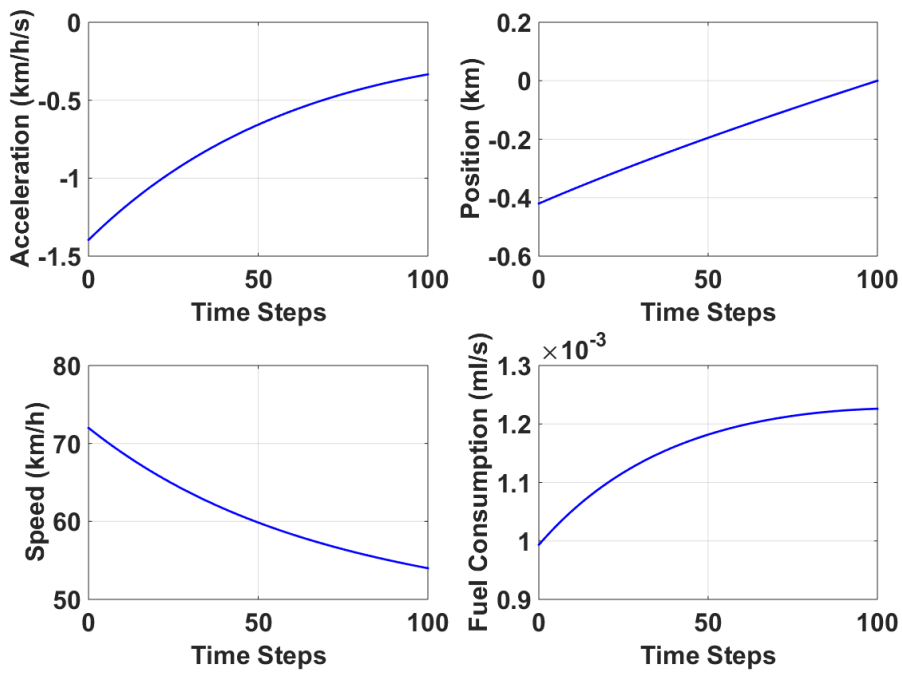


Figure 7: Graphical representation of the optimal solution, regarding the minimisation of the approximated fuel consumption model for scenario 4.

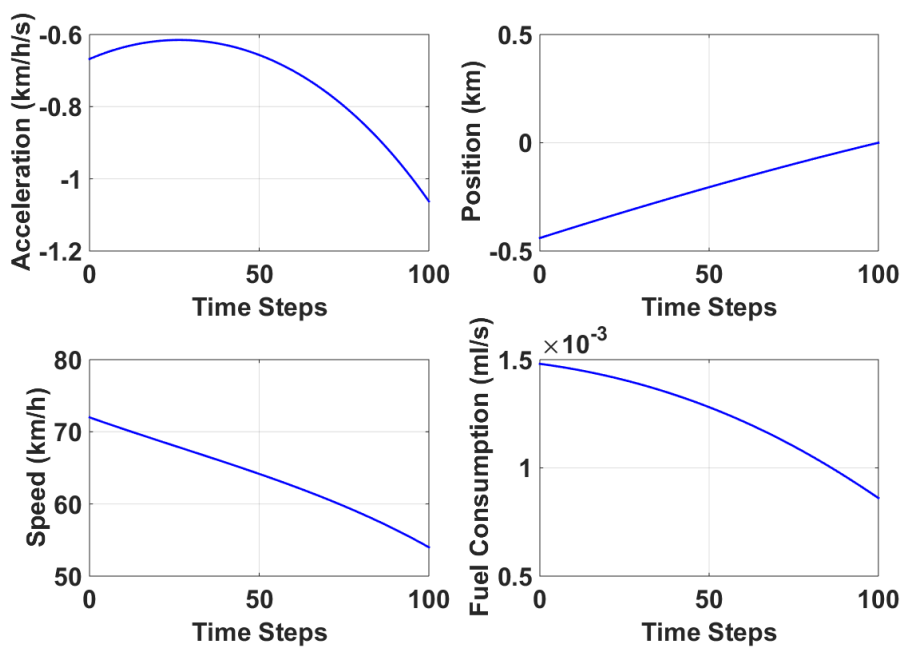


Figure 8: Graphical representation of the optimal solution, regarding the minimisation of the approximated fuel consumption model for scenario 5.

4.2 A Numerical Solution of the Fuel Consumption Model

In this section, we give a numerical solution of the reformulated problem into the Mayer form, introducing an extra state variable, y , defined by the differential equation

$$\dot{y} = f(v, a)$$

where $f(v, a)$ is the ARRB fuel consumption model, with initial condition $y(0) = 0$. The formulation becomes as follows:

$$\left\{ \begin{array}{l} \min \int_0^T f(v, a) dt \\ \text{s.t.} \\ \dot{x} = v \\ \dot{v} = a \\ \\ x(0) = x_0, \quad x(T) = 0 \\ v(0) = v_0, \quad v(T) = v_e \end{array} \right. \implies \left\{ \begin{array}{l} \min y(T) \\ \text{s.t.} \\ \dot{x} = v \\ \dot{v} = a \\ \dot{y} = f(v, a) \\ \\ x(0) = x_0, \quad x(T) = 0 \\ v(0) = v_0, \quad v(T) = v_e \\ y(0) = 0 \end{array} \right.$$

Firstly, a piecewise-constant control profile parameterization over n steps is considered as follows,

$$u(t) = a^k, \quad t_{k-1} \leq t \leq t_k, \quad k = 1, \dots, n,$$

with the time steps being equally spaced, and then a piecewise-linear parameterization is applied for the control profile.

For the purposes of the problem, the number of stages n is set equal to 9, while the initial control values are $a^k = 1 \quad k = 1, \dots, n$. For the integration of the differential equations, we have used the MatLab function `ode45` and for the optimization the function `fmincon` using the interior-point algorithm.

Figure 5.4.1 describes the algorithmic procedure in a simple flow diagram form and in Figures 10 - 14 and Figures 15 - 19 are shown the obtained results of the piecewise constant

and piecewise linear cases respectively with the same initial conditions as those of the analytic solution.

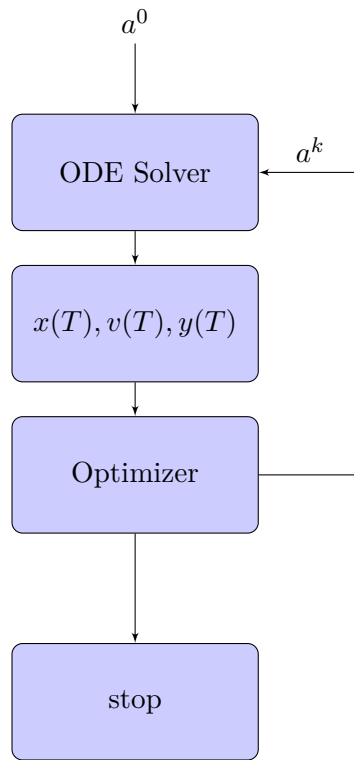


Figure 9: Flow Chart

4.2.1 Piecewise Constant Solution

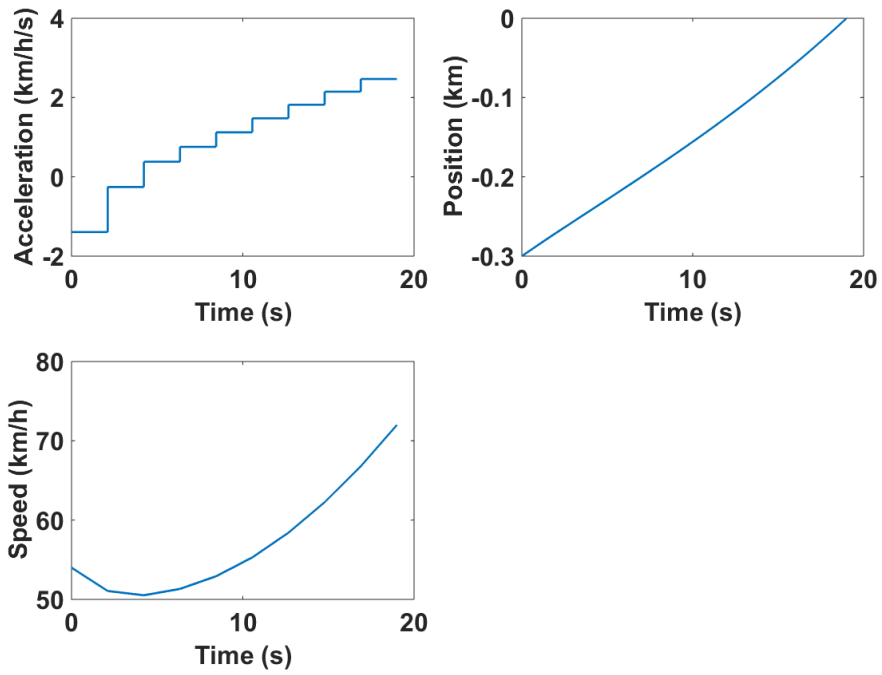


Figure 10: Control and states diagrams for the Piecewise-Constant solution for Scenario

1

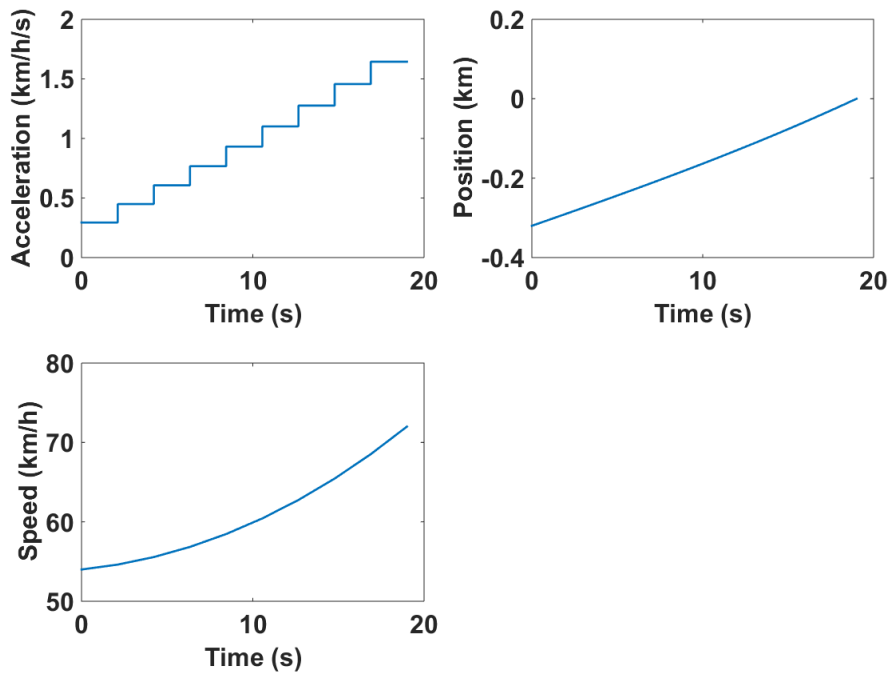


Figure 11: Control and states diagrams for the Piecewise-Constant solution for Scenario

2

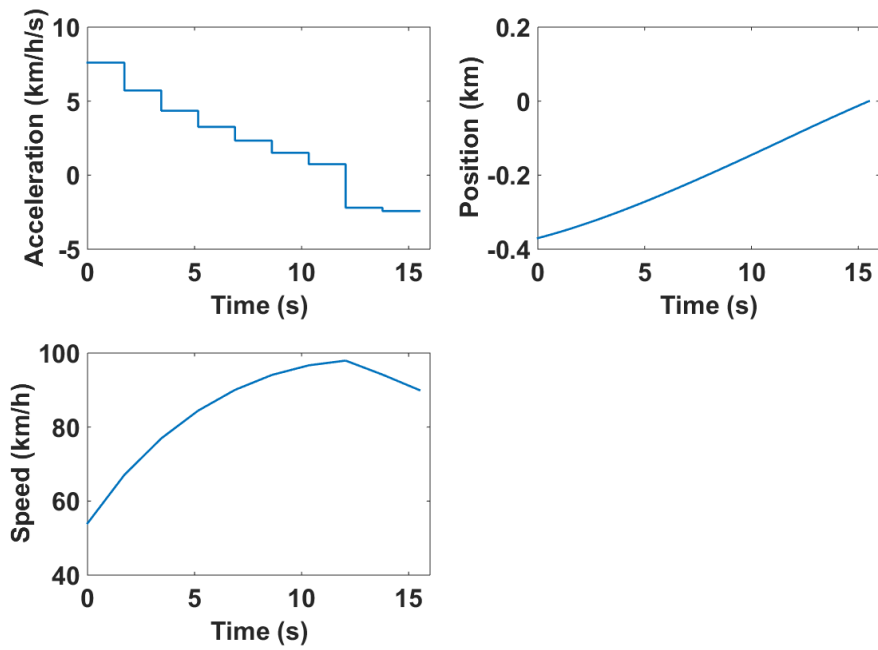


Figure 12: Control and states diagrams for the Piecewise-Constant solution for Scenario

3

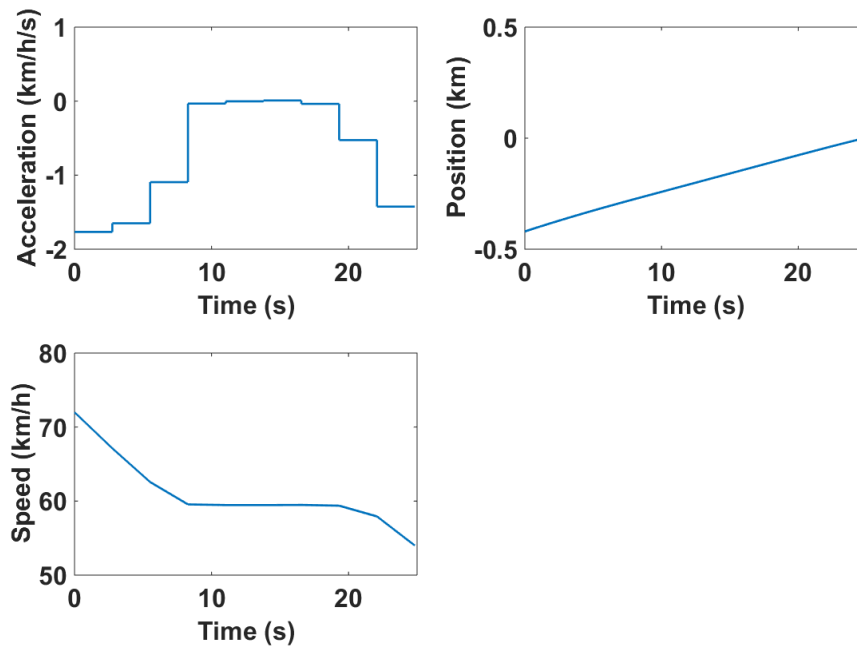


Figure 13: Control and states diagrams for the Piecewise-Constant solution for Scenario

4

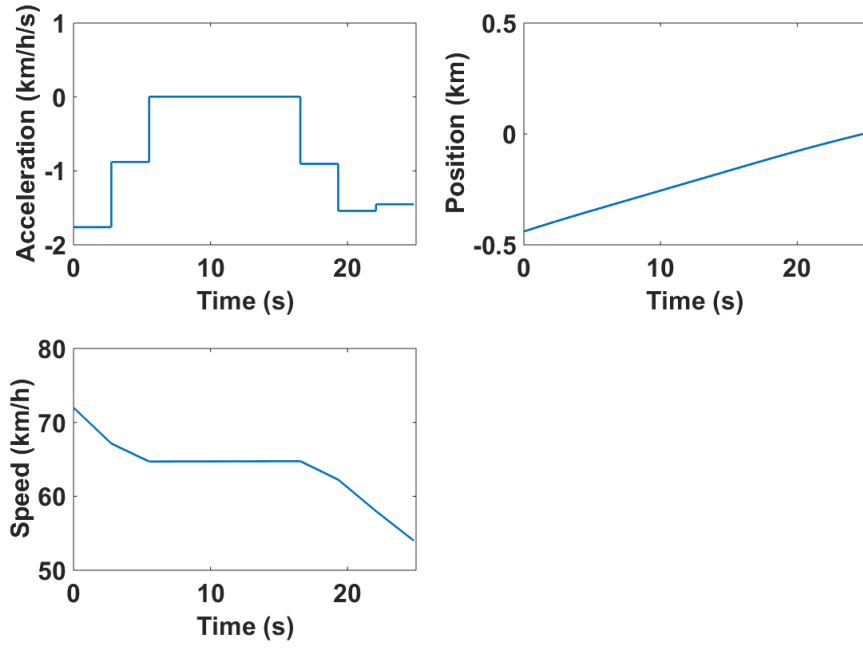


Figure 14: Control and states diagrams for the Piecewise-Constant solution for Scenario 5

4.2.2 Piecewise Linear Interpolation Solution

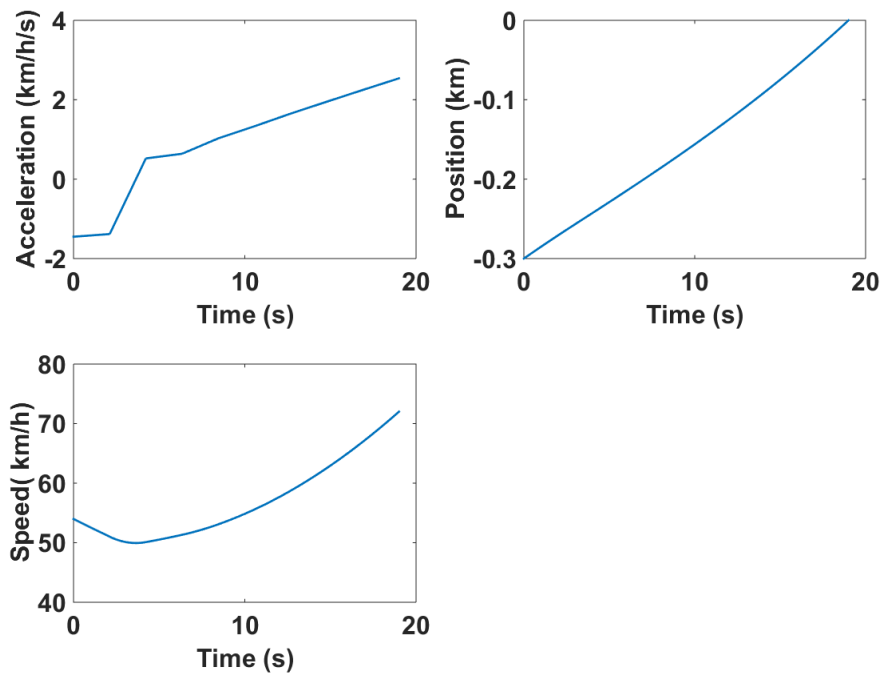


Figure 15: Control and states diagrams for the Piecewise-Linear solution for Scenario 1

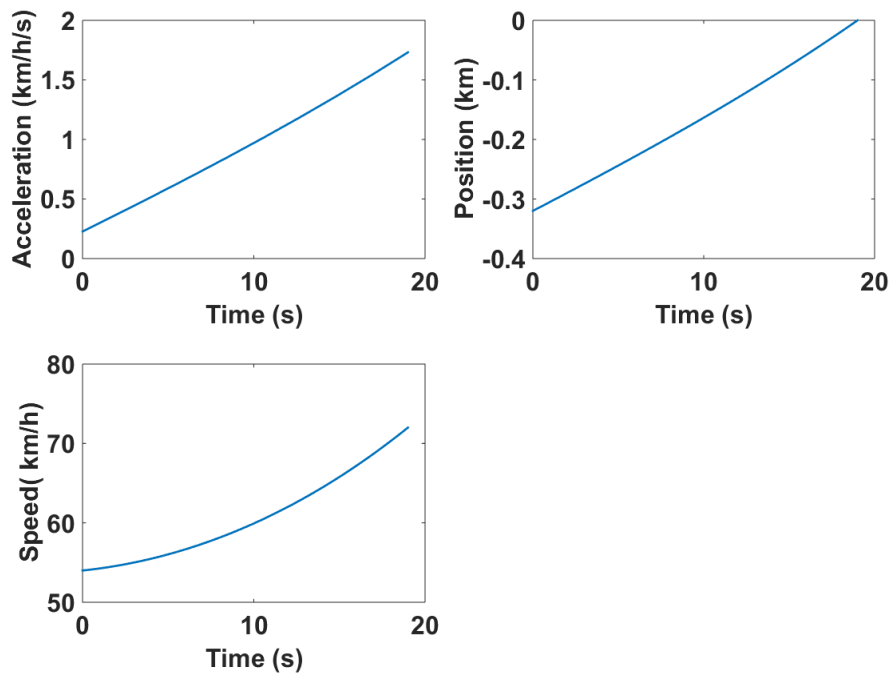


Figure 16: Control and states diagrams for the Piecewise-Linear solution for Scenario 2

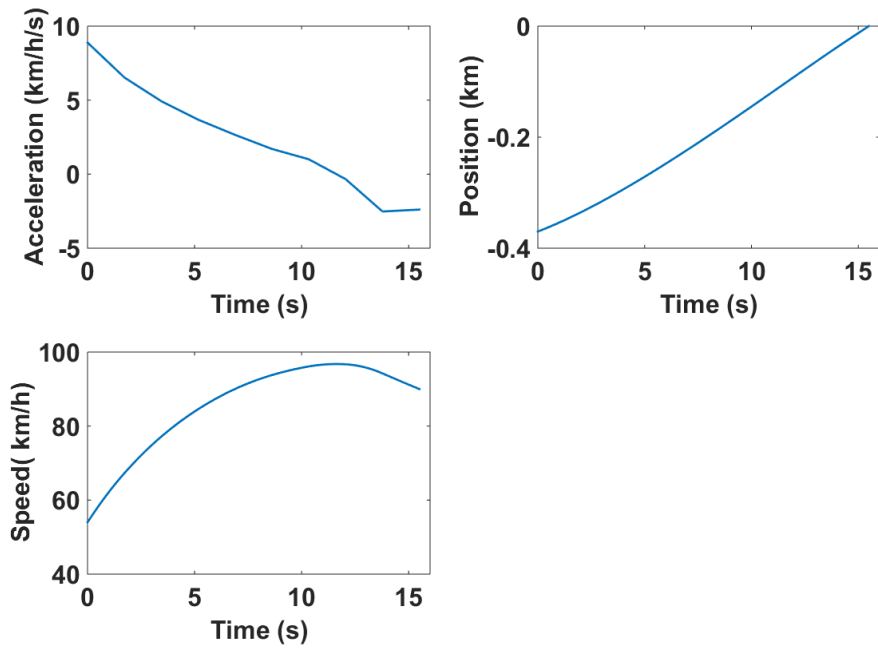


Figure 17: Control and states diagrams for the Piecewise-Linear solution for Scenario 3

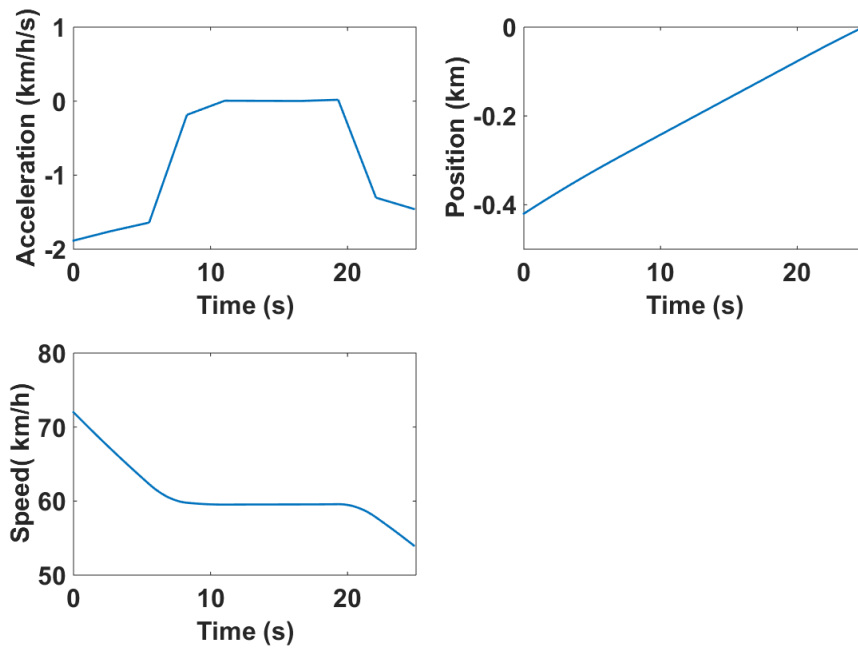


Figure 18: Control and states diagrams for the Piecewise-Linear solution for Scenario 4

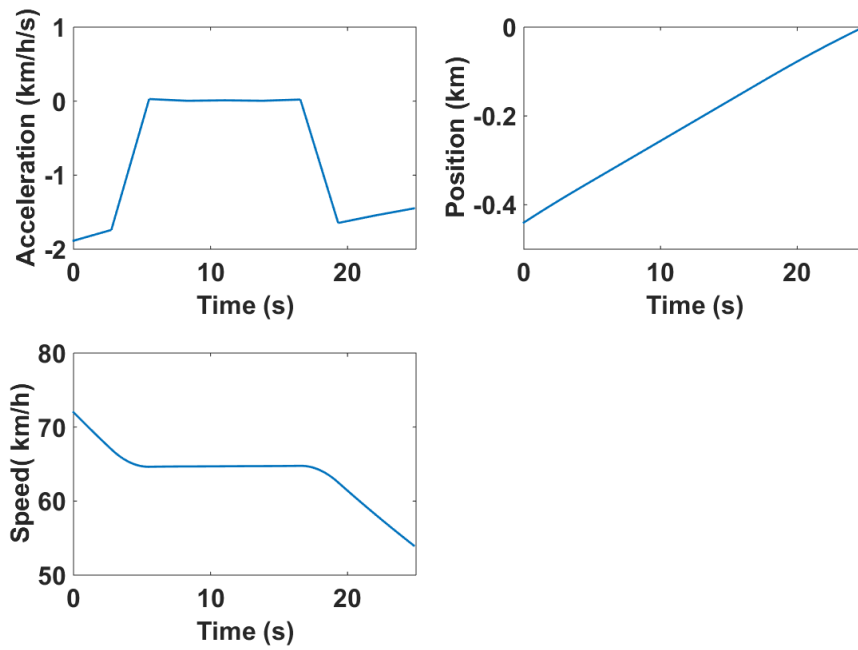


Figure 19: Control and states diagrams for the Piecewise-Linear solution for Scenario 5

4.3 Feasible Direction Algorithm

Tables 1 - 4 show the obtained results of different initial conditions of the problem (Scenarios 1-2, 4-5) for penalty terms $p_1 = 10^2$ and $p_2 = 10^3$, with different search direction methods and $\varepsilon = 10^{-5}$. As an initial guess, the trajectory $u(k) = 0 \text{ m/s}^2, \forall k \in [0, 99]$ was utilized. Figures 20-23 shows the decrease of cost function values in dependence of the computing time during employment of the numerical algorithm with different direction methods and the evolution of the control and states trajectories $u(k), x_1(k), x_2(k)$. From these results we may draw the following conclusions:

- All methods converge, despite the bad initial guess, to the optimal solution.
- For the chosen penalties and initial guess of the trajectory $u(k)$, the conjugate gradient methods are the most efficient.
- The PR method is most efficient in the majority of our scenarios, whilst FR and DFP are approximately equally efficient. RPROP and ARCprop converge quite fast and efficient despite the many iterations needed in order to reach the optimum.
- In all cases, the final conditions are reached with sufficient accuracy.

	$p_1 = 10^2, p_2 = 10^3$				
	Iterations	CPU-s	$x_1(T)$	$x_2(T)$	cost
Steepest Descent	21	0.39	-0.000059	19.997863	41.4192
DFP	21	0.46	-0.000103	19.997874	41.4202
BFGS	15	0.08	-0.000102	19.997874	41.4201
Fletcher-Reeves	4	0.02	-0.000267	19.997890	41.4222
Polak-Ribierre	4	0.02	-0.000214	19.997883	41.4217
RPROP	534	1.50	-0.000327	19.978779	41.4184
ARCprop	25	0.03	-0.000327	19.978779	41.4186

Table 1: Comparison of search direction methods for Scenario 1

	$p_1 = 10^2, p_2 = 10^3$				
	Iterations	CPU-s	$x_1(T)$	$x_2(T)$	cost
Steepest Descent	11	0.64	-0.002979	19.998153	42.0145
DFP	4	0.01	-0.002812	19.998168	42.0142
BFGS	11	0.26	-0.002812	19.998168	42.0142
Fletcher-Reeves	4	0.03	-0.002812	19.998168	42.0146
Polak-Ribierre	3	0.02	-0.002772	19.998172	42.0150
RPROP	286	1.22	-0.002757	19.981542	42.0148
ARCprop	19	0.09	-0.002757	19.981542	42.0148

Table 2: Comparison of search direction methods for Scenario 2

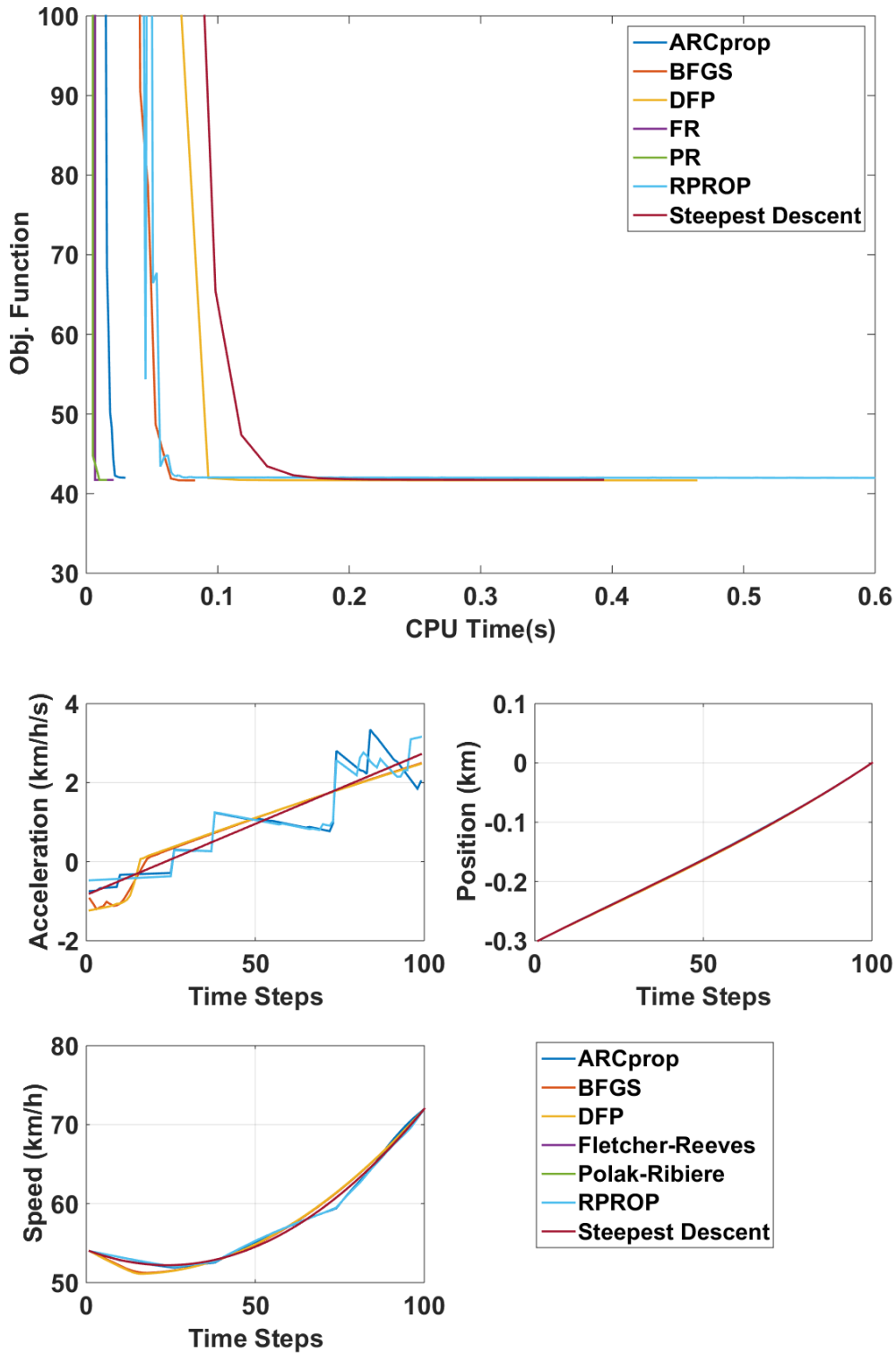


Figure 20: Objective function decrease in dependence of the computing time and evolution of control and states, in dependence of the number of time steps for Scenario 1

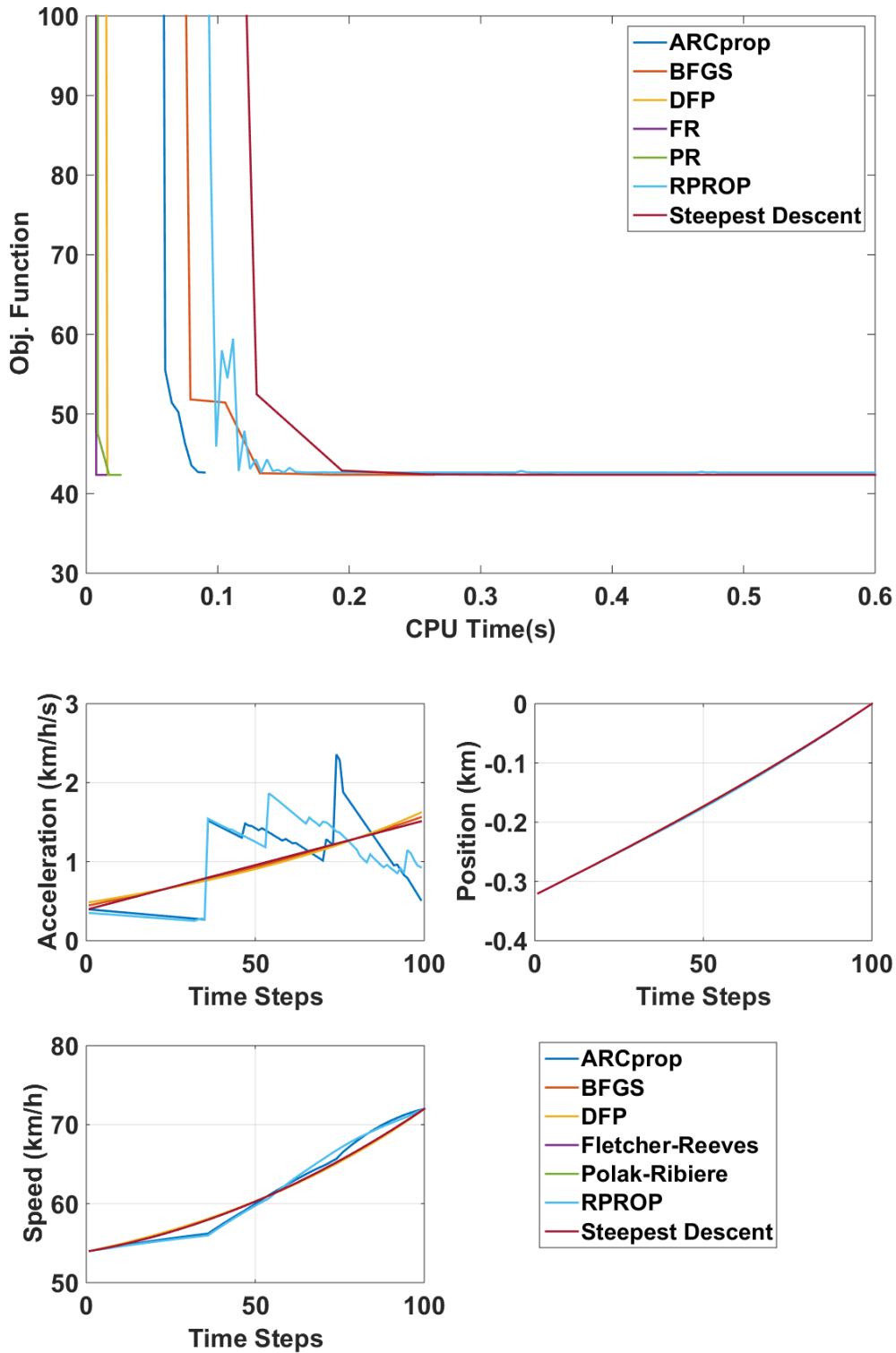


Figure 21: Objective function decrease in dependence of the computing time and evolution of control and states, in dependence of the number of time steps for Scenario 2

	$p_1 = 10^2, p_2 = 10^3$				
	Iterations	CPU-s	$x_1(T)$	$x_2(T)$	cost
Steepest Descent	5	0.02	-0.004217	14.999324	28.7669
DFP	20	0.14	-0.004201	14.999322	28.7514
BFGS	20	0.13	-0.004201	14.999322	28.7511
Fletcher-Reeves	3	0.05	-0.003998	14.999288	28.7682
Polak-Ribierre	3	0.05	-0.004051	14.999305	28.7689
RPROP	56	0.2	-0.003985	14.992897	28.7744
ARCprop	19	0.08	-0.003985	14.992897	28.7748

Table 3: Comparison of search direction methods for Scenario 4

	$p_1 = 10^2, p_2 = 10^3$				
	Iterations	CPU-s	$x_1(T)$	$x_2(T)$	cost
Steepest Descent	5	0.03	-0.004310	14.999300	30.8585
DFP	20	0.14	-0.004510	14.999328	30.8481
BFGS	20	0.13	-0.004510	14.999328	30.8484
Fletcher-Reeves	5	0.08	-0.004526	14.999329	30.8627
Polak-Ribierre	2	0.03	-0.004344	14.999312	30.8647
RPROP	52	0.2	-0.004436	14.993173	30.8770
ARCprop	33	0.12	-0.004436	14.993173	30.8770

Table 4: Comparison of search direction methods for Scenario 5

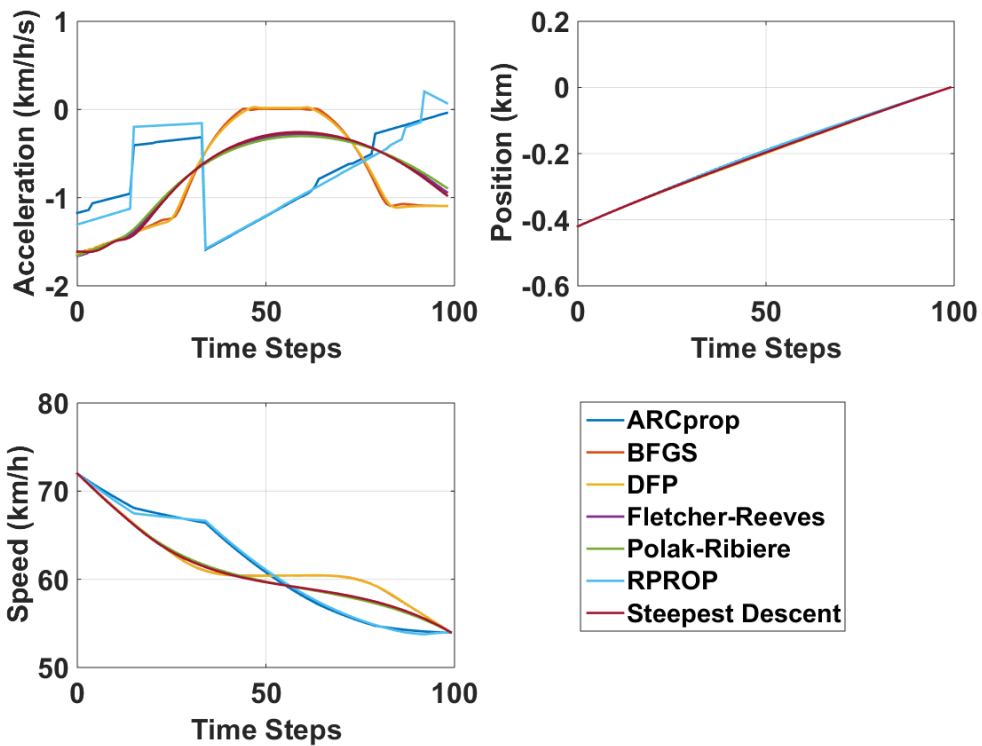
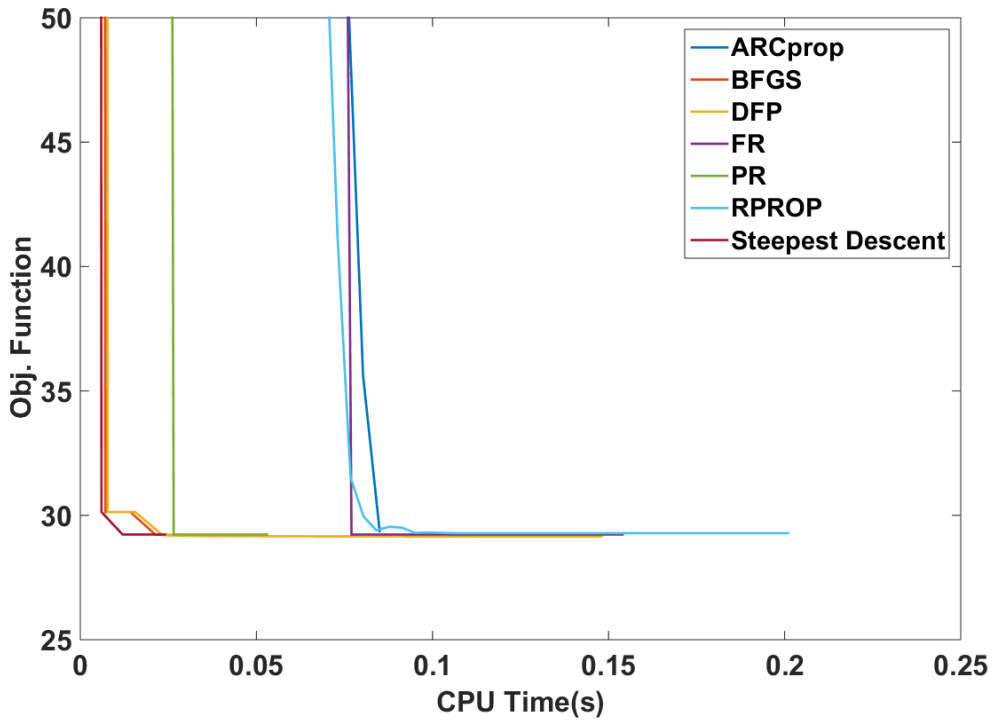


Figure 22: Objective function decrease in dependence of the computing time and evolution of control and states, in dependence of the number of time steps for Scenario 4

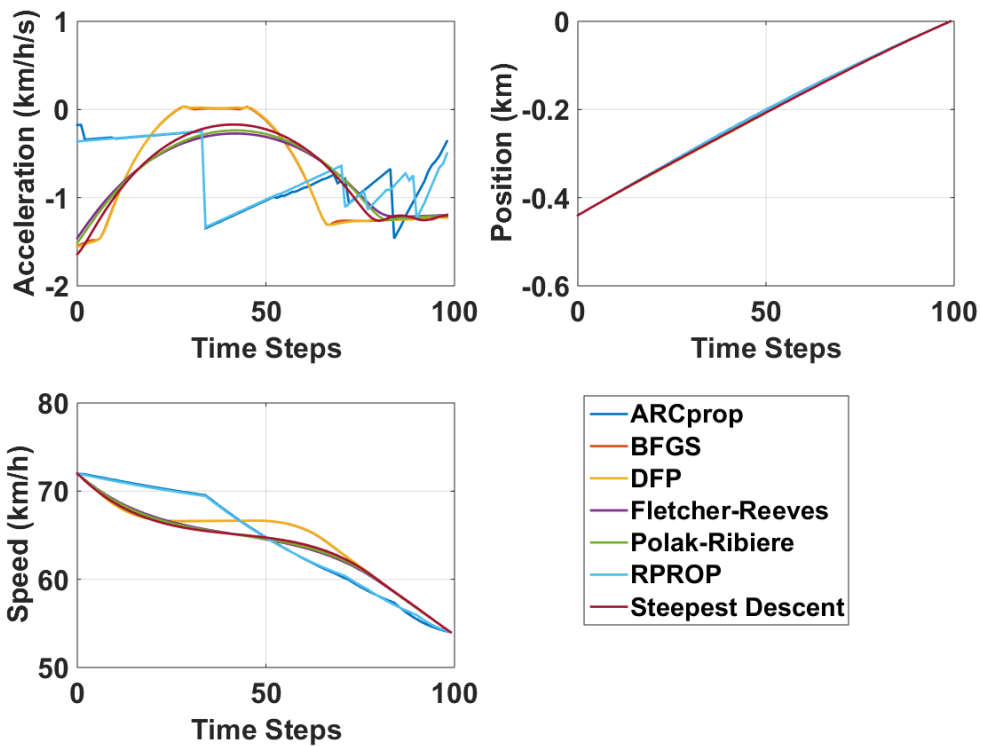
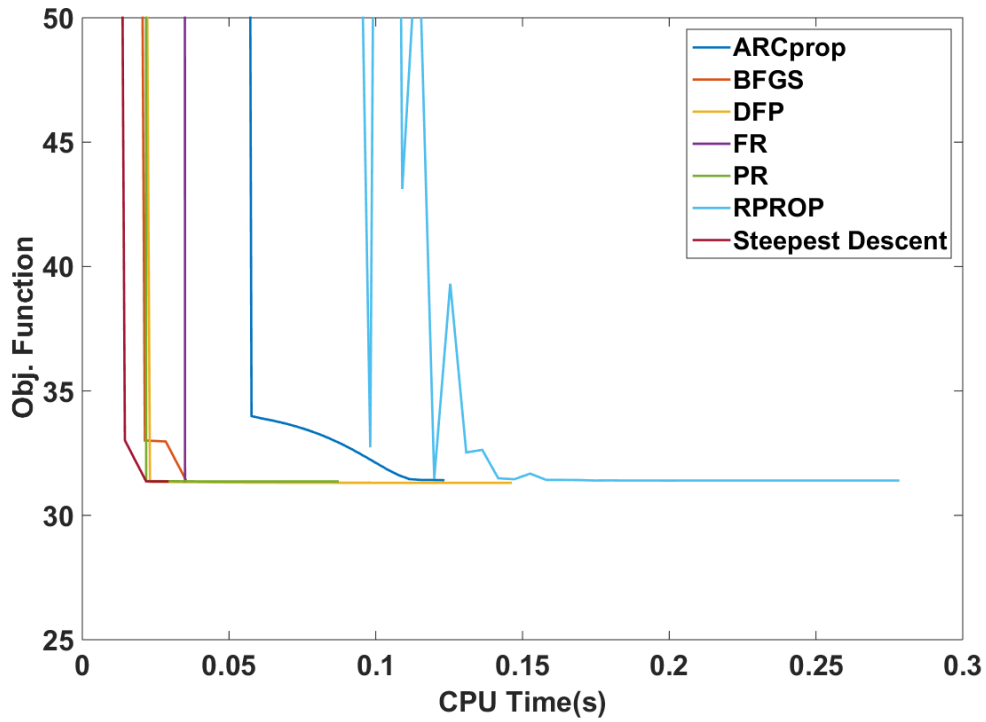


Figure 23: Objective function decrease in dependence of the computing time and evolution of control and states, in dependence of the number of time steps for Scenario 5

4.4 Fuel Consumption Comparison for Different Time Step and Same Time Horizon Cases

In this section we compare the fuel consumption value obtained from the search direction methods for the same time horizon but different time steps for each of our scenarios. The smaller we set the number of time steps, the less computational time is needed for the algorithms to converge to the optimal solution but also the less accurate is the solution. Thus, if the the percentage difference between the fuel consumption obtained from bigger to smaller time steps is small (e.g. less than 1%), we can assume that we can use a reasonably small number of time steps without losing accuracy in our optimal solution. In Tables 5-9, we present the obtained fuel consumption of Scenarios 1-5 for time steps 50, 100, 200, 400, 800. Case 1 describes the optimal fuel consumption obtained with the number of time steps, as we set it to the algorithm, while case 2 is the optimal fuel consumption based on an equivalent optimal control trajectory of 800 time steps, of the optimal control trajectory obtained from the algorithm.

Fuel Consumption (ml)	Case 1	Case 2	Analytic Solution
25s \rightarrow 50 steps	41.4037	41.5851	
25s \rightarrow 100 steps	41.4201	41.5830	
25s \rightarrow 200 steps	41.5377	41.5740	
25s \rightarrow 400 steps	41.5453	41.5574	
25s \rightarrow 800 steps	41.5323	41.5323	41.6435

Table 5: Fuel Consumption based on the ARRB fuel consumption model for the same time horizon situation and different number of time steps for the scenario 1

Fuel Consumption (ml)	Case 1	Case 2	Analytic Solution
25s → 50 steps	42.0037	42.1385	
25s → 100 steps	42.0142	42.1351	
25s → 200 steps	42.1015	42.1285	
25s → 400 steps	42.1062	42.1152	
25s → 800 steps	42.0889	42.0889	

Table 6: Fuel Consumption based on the ARRB fuel consumption model for the same time horizon situation and different number of time steps for the scenario 2

Fuel Consumption (ml)	Case 1	Case 2	Analytic Solution
25s → 50 steps	81.6817	82.4299	
25s → 100 steps	82.0533	82.4138	
25s → 200 steps	82.2409	82.3899	
25s → 400 steps	82.2942	82.3438	
25s → 800 steps	82.2519	82.2519	

Table 7: Fuel Consumption based on the ARRB fuel consumption model for the same time horizon situation and different number of time steps for the scenario 3

Fuel Consumption (ml)	Case 1	Case 2	Analytic Solution
25s → 50 steps	28.8017	28.7248	
25s → 100 steps	28.7511	28.7262	
25s → 200 steps	28.7409	28.7251	
25s → 400 steps	28.7413	28.7356	
25s → 800 steps	28.7240	28.7240	

Table 8: Fuel Consumption based on the ARRB fuel consumption model for the same time horizon situation and different number of time steps for the scenario 4

Fuel Consumption (ml)	Case 1	Case 2	Analytic Solution
25s → 50 steps	30.8984	30.8218	
25s → 100 steps	30.8484	30.8219	
25s → 200 steps	30.8391	30.8225	
25s → 400 steps	30.8232	30.8178	
25s → 800 steps	30.8195	30.8195	

Table 9: Fuel Consumption based on the ARRB fuel consumption model for the same time horizon situation and different number of time steps for the scenario 5

4.5 Fuel Consumption Comparison for the Same Time Step and Different Time Horizon Cases

In this section we compare the fuel consumption value obtained from the search direction methods for the same time step but different time horizon for each one of our scenarios. In this case, we want to check if the approximation of the fuel consumption optimal problem is getting better, as we have more time (therefore more options) to lead the initial states to the final states. In Figures 24-38, we show the control and the states of Scenarios 1-5 for time steps 100, 200, 300 (KMAX in the figures) and multiplying time horizon two and three times ($T = 2 \cdot T$ and $T = 3 \cdot T$) accordingly, in order to achieve the same time step in each case.

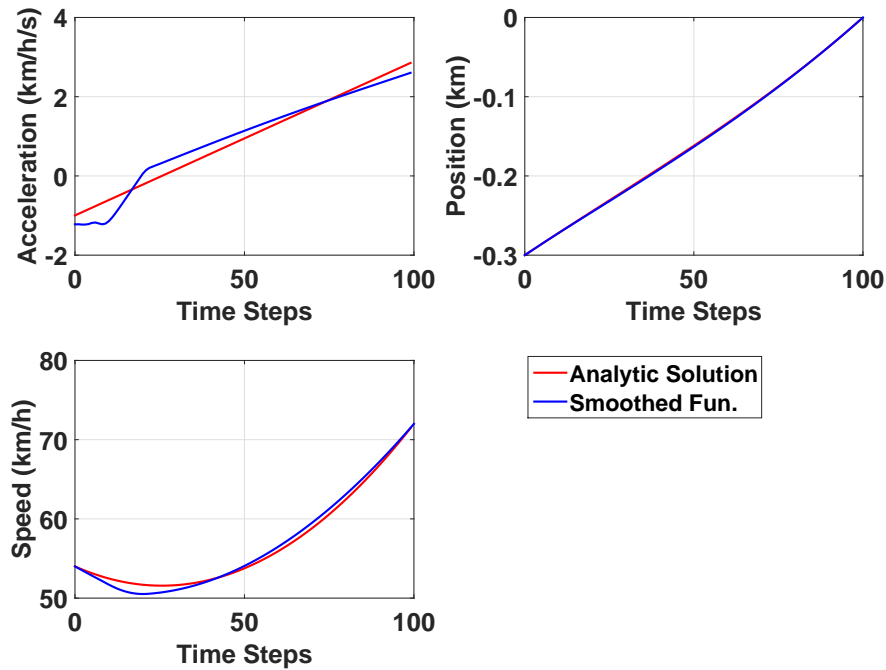


Figure 24: Controls and states of the analytic solution of the approximated fuel consumption model and the smoothed fuel consumption model for the case of $T = 19$ s and $KMAX = 100$ for Scenario 1

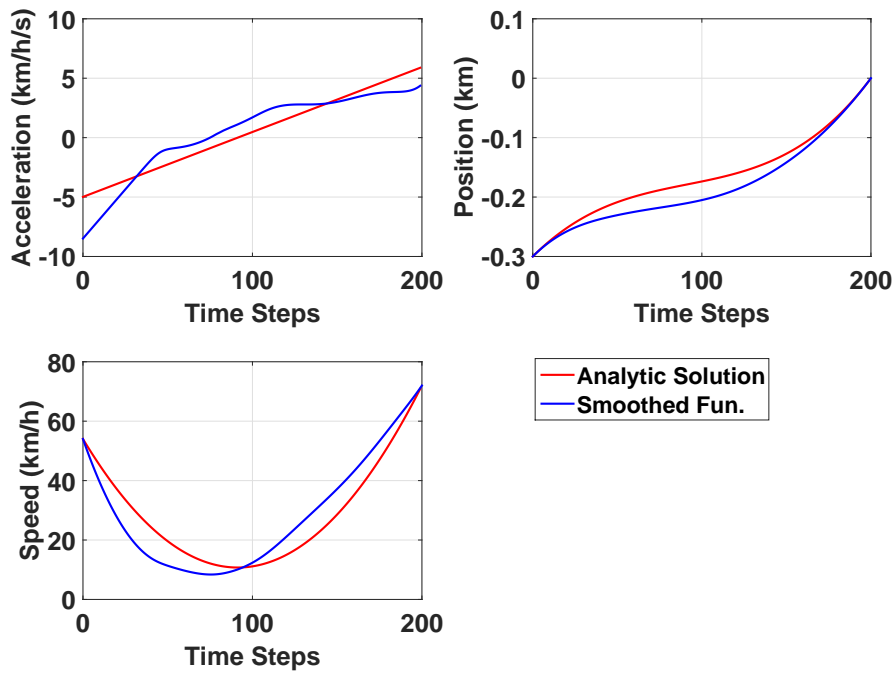


Figure 25: Controls and states of the analytic solution of the approximated fuel consumption model and the smoothed fuel consumption model for the case of $T = 38s$ and $KMAX=200$ for Scenario 1

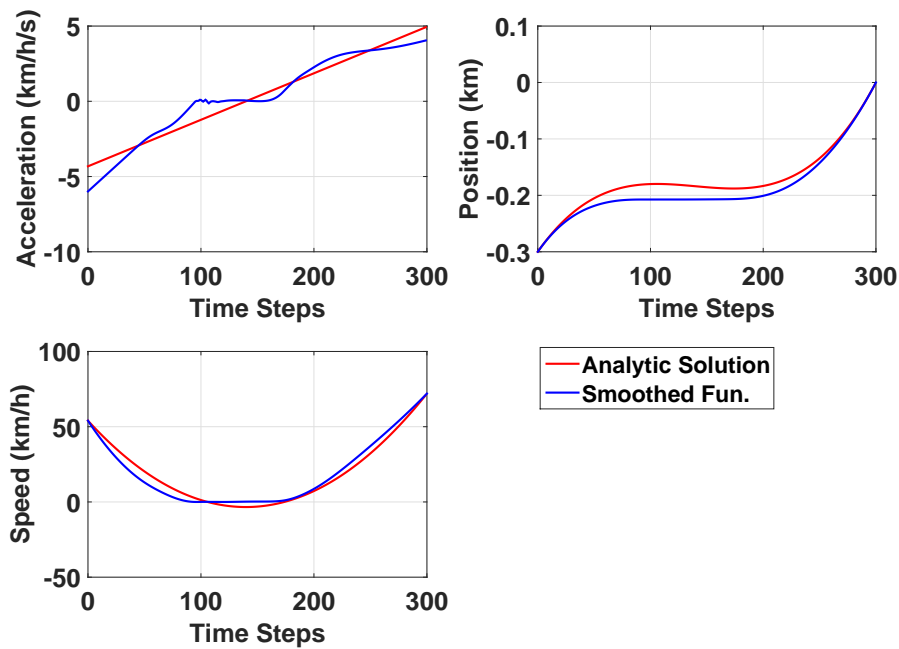


Figure 26: Controls and states of the analytic solution of the approximated fuel consumption model and the smoothed fuel consumption model for the case of $T = 57s$ and $KMAX=300$ for Scenario 1

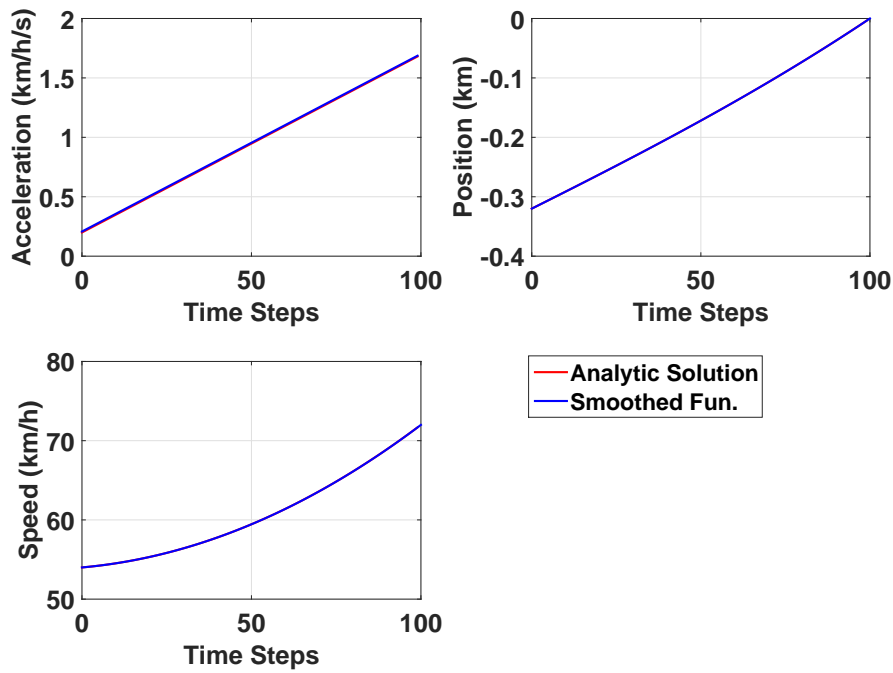


Figure 27: Controls and states of the analytic solution of the approximated fuel consumption model and the smoothed fuel consumption model for the case of $T = 19$ s and $KMAX=100$ for Scenario 2

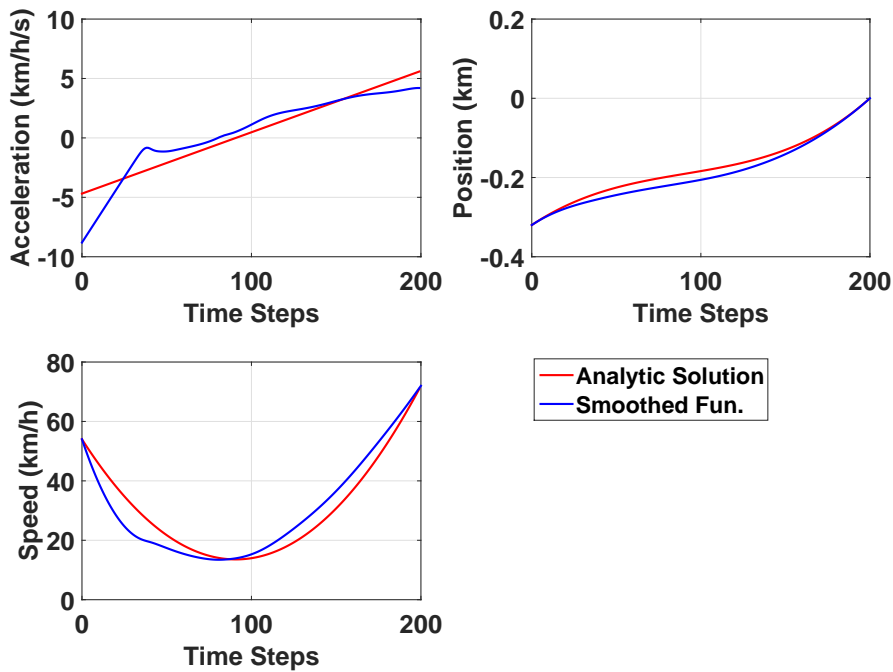


Figure 28: Controls and states of the analytic solution of the approximated fuel consumption model and the smoothed fuel consumption model for the case of $T = 38$ s and $KMAX=200$ for Scenario 2

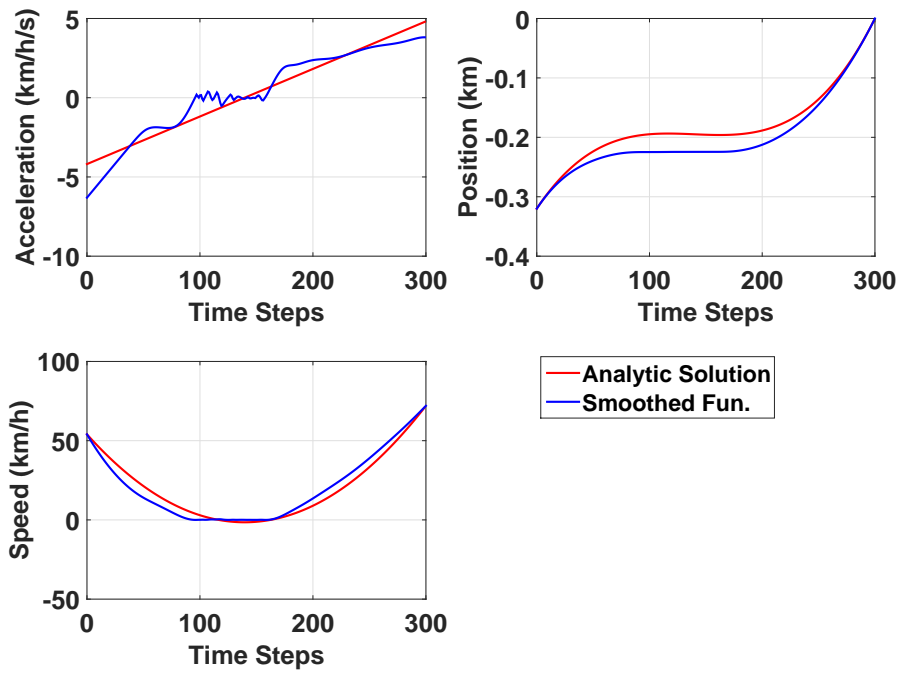


Figure 29: Controls and states of the analytic solution of the approximated fuel consumption model and the smoothed fuel consumption model for the case of $T = 57s$ and $KMAX=300$ for Scenario 2

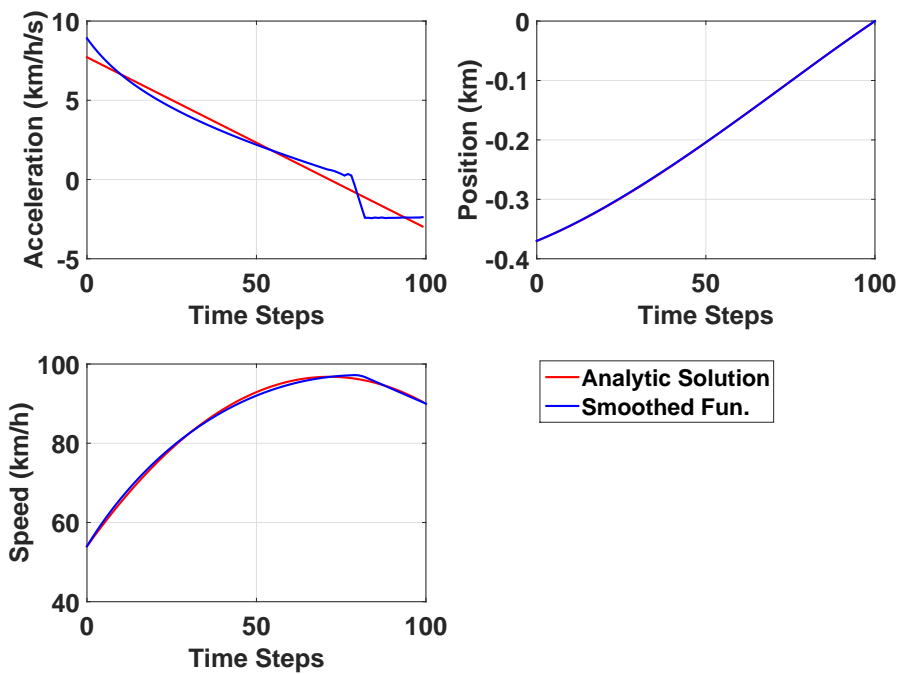


Figure 30: Controls and states of the analytic solution of the approximated fuel consumption model and the smoothed fuel consumption model for the case of $T = 15.5s$ and $KMAX=100$ for Scenario 3

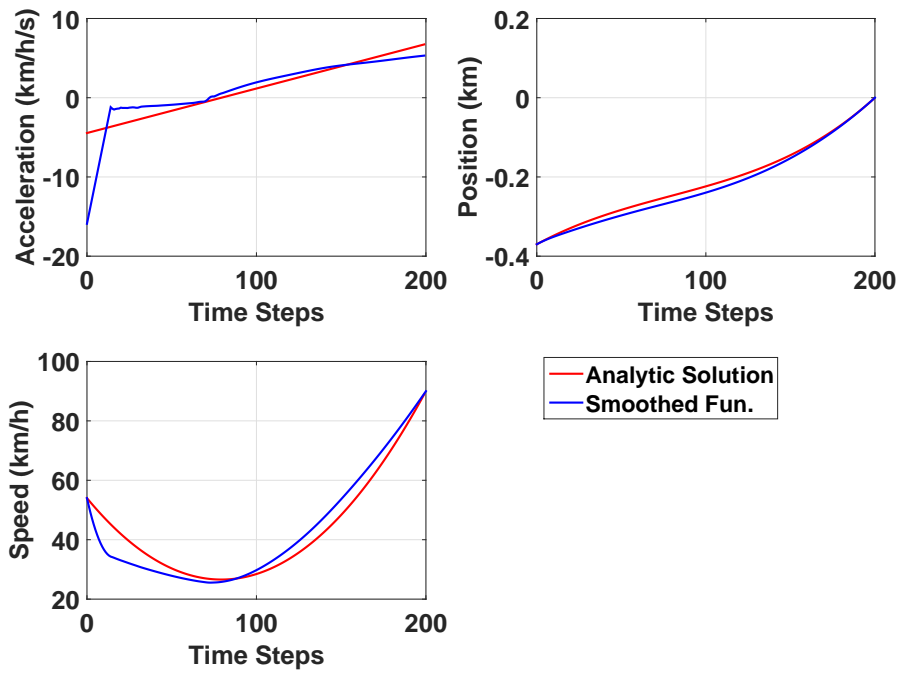


Figure 31: Controls and states of the analytic solution of the approximated fuel consumption model and the smoothed fuel consumption model for the case of $T = 31s$ and $KMAX=200$ for Scenario 3

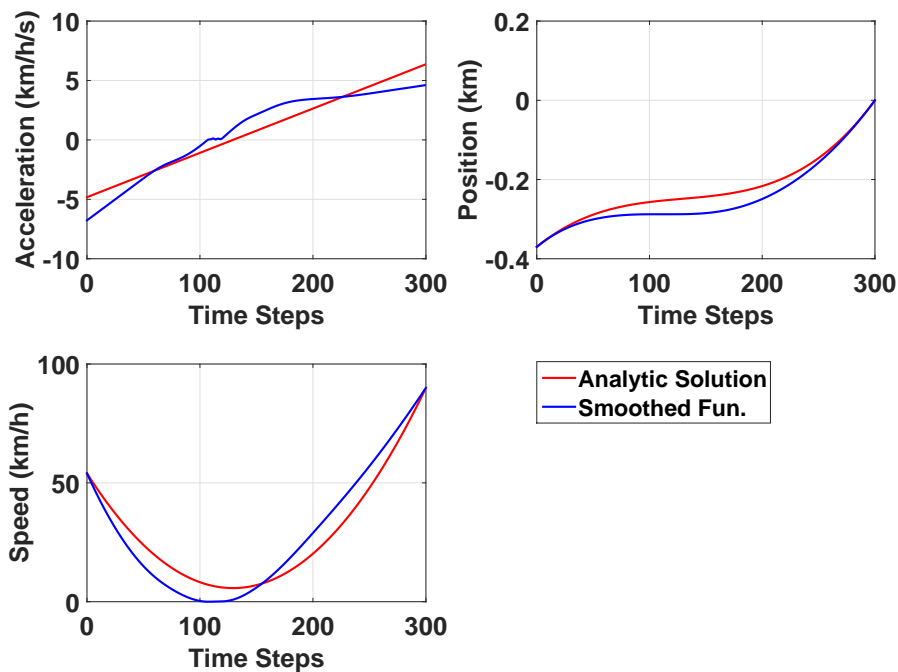


Figure 32: Controls and states of the analytic solution of the approximated fuel consumption model and the smoothed fuel consumption model for the case of $T = 46.5s$ and $KMAX=300$ for Scenario 3

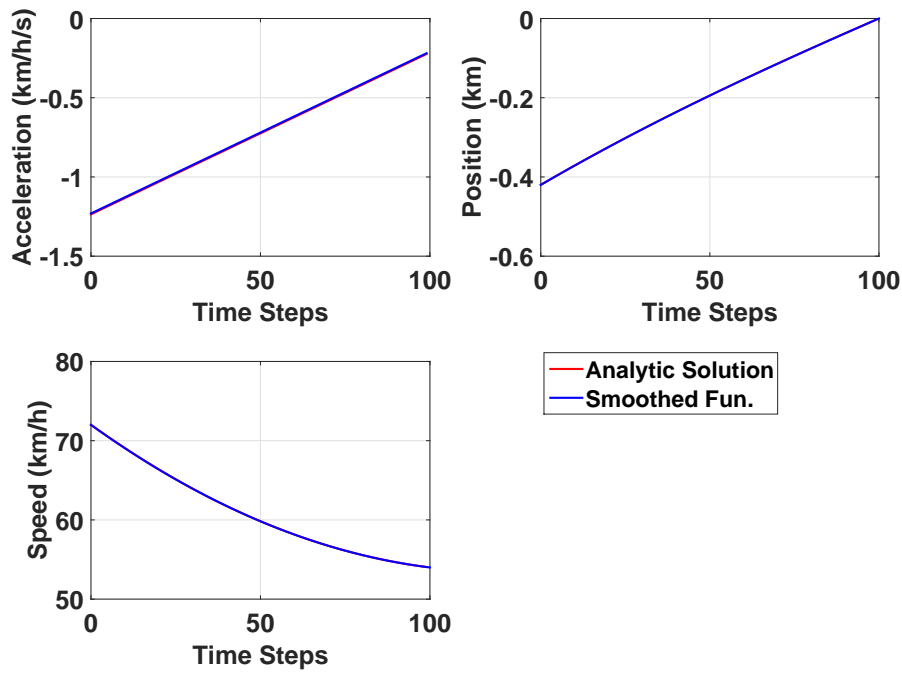


Figure 33: Controls and states of the analytic solution of the approximated fuel consumption model and the smoothed fuel consumption model for the case of $T = 25$ s and $KMAX=100$ for Scenario 4

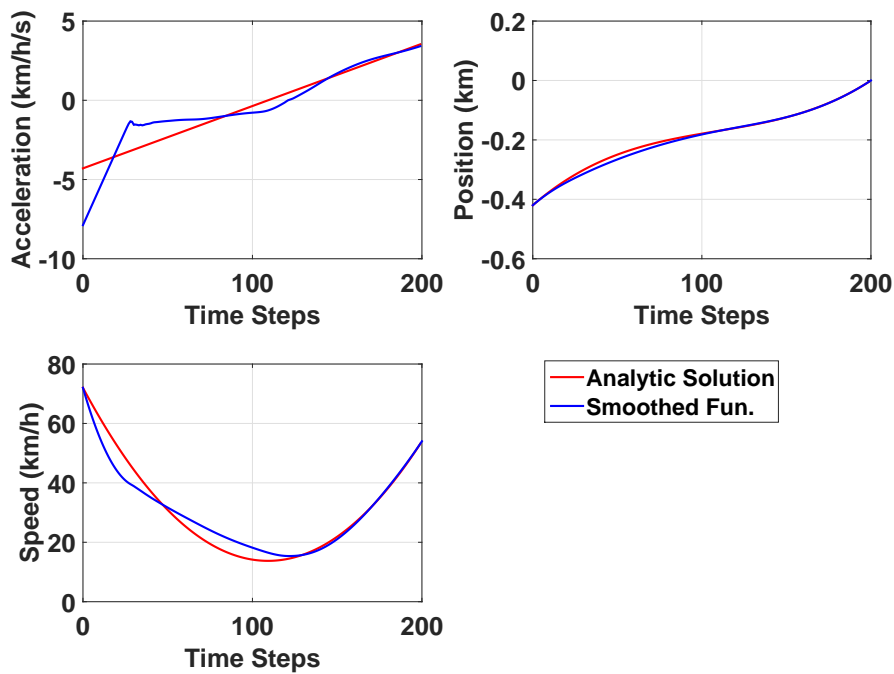


Figure 34: Controls and states of the analytic solution of the approximated fuel consumption model and the smoothed fuel consumption model for the case of $T = 50$ s and $KMAX=200$ for Scenario 4

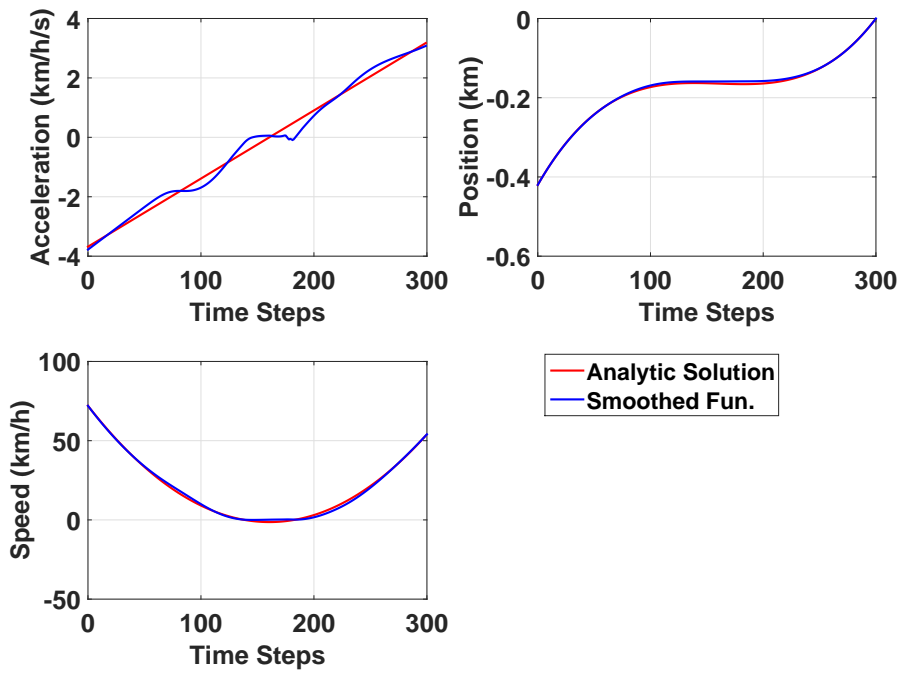


Figure 35: Controls and states of the analytic solution of the approximated fuel consumption model and the smoothed fuel consumption model for the case of $T = 75s$ and $KMAX=300$ for Scenario 4

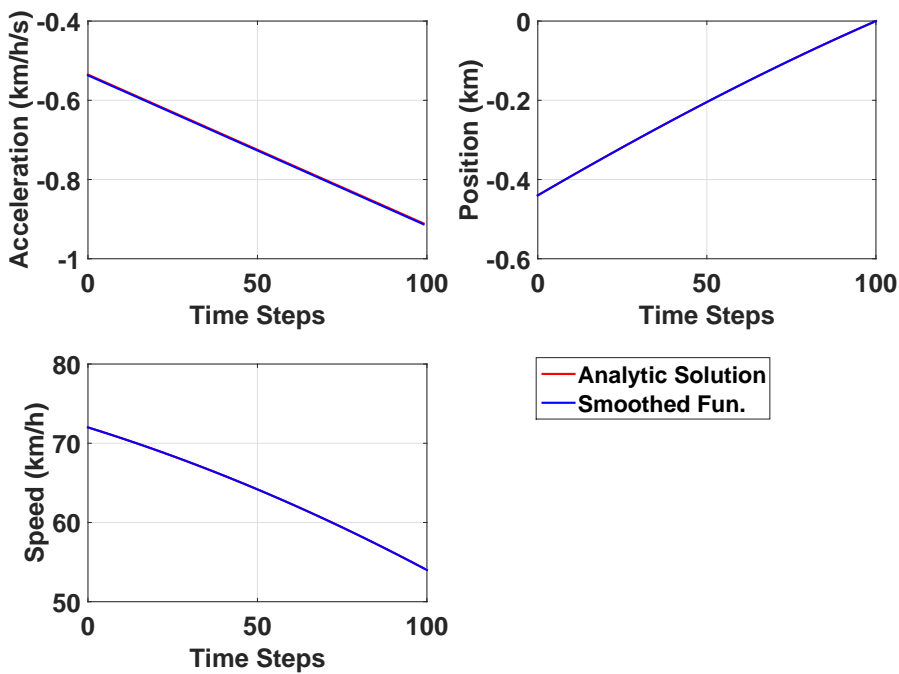


Figure 36: Controls and states of the analytic solution of the approximated fuel consumption model and the smoothed fuel consumption model for the case of $T = 25s$ and $KMAX=100$ for Scenario 5

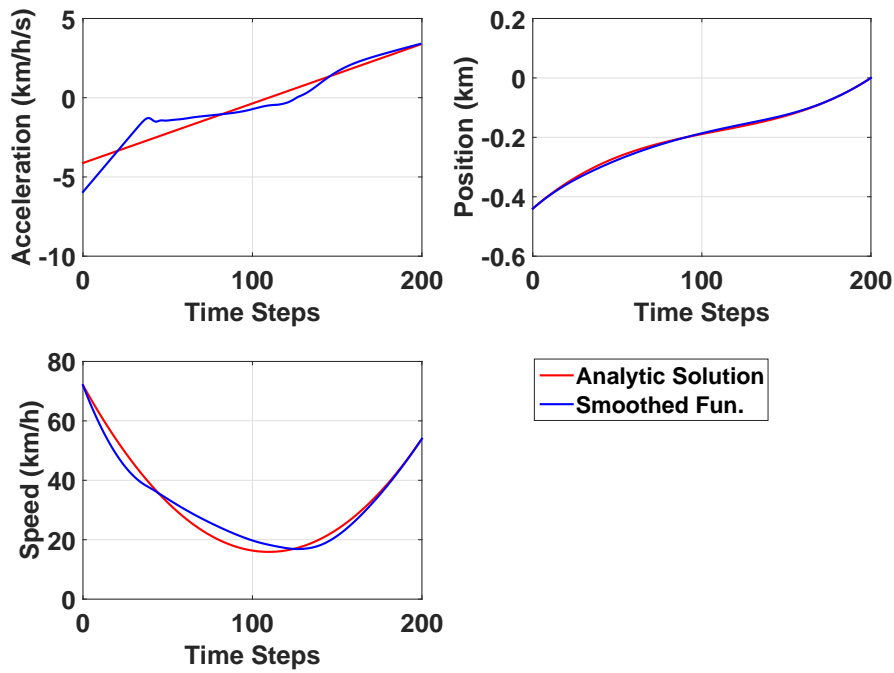


Figure 37: Controls and states of the analytic solution of the approximated fuel consumption model and the smoothed fuel consumption model for the case of $T = 50$ s and $KMAX=200$ for Scenario 5

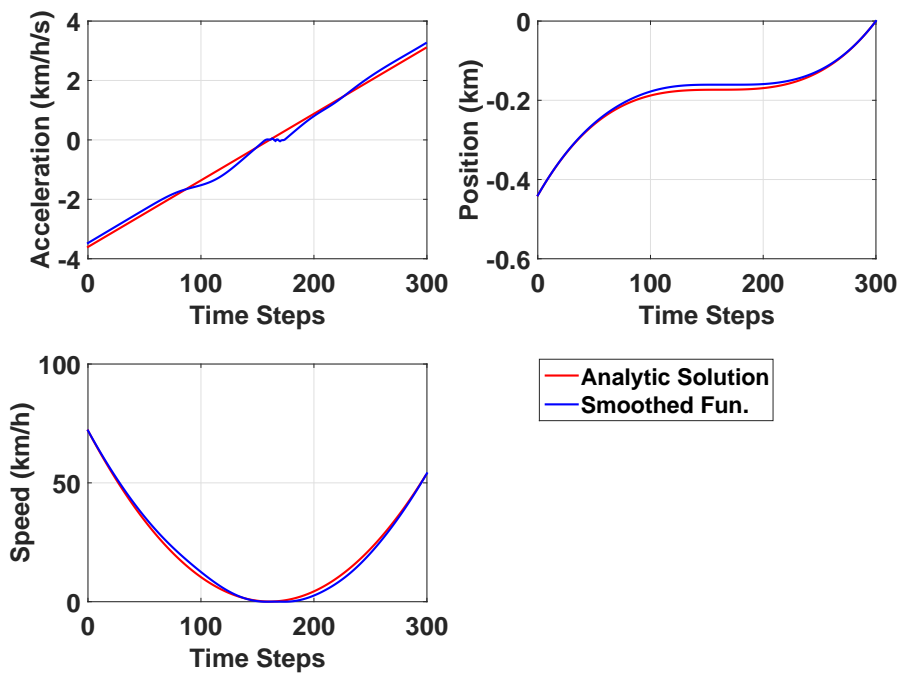


Figure 38: Controls and states of the analytic solution of the approximated fuel consumption model and the smoothed fuel consumption model for the case of $T = 75$ s and $KMAX=300$ for Scenario 5

5

Comparison Between Analytic Solution of Fuel Consumption's Model Approximation and Numerical Solutions

In this chapter, we compare the results from the analytic solution of the minimisation of the fuel's consumption function approximation and the minimisation of the ARRB fuel consumption model using the numerical solutions of section 4.2 and chapter 2.4. Furthermore, as in bibliography is proposed, there is a positive correlation between acceleration and fuel consumption. So it was rational to solve the described problem using as cost function the $\frac{1}{2}u^2$ (e.g. [Malikopoulos et al. \(2016\)](#)) and compare the results with those of the approximated and the smoothed fuel consumption model. This comparison would show us if the minimisation of the square of the acceleration is a good approach for eco-driving problems, compared to the minimisation of an approximated fuel consumption model.

Figures 39-43 show the control and the states of analytic solution of the Taylor approximation of the fuel consumption, the feasible direction algorithm (using the BFGS algorithm), the piecewise-constant method and the function $\frac{1}{2}u^2$ as cost function, versus time steps and Tables 10-14 show the obtained optimal solution of each method. From the results, we can notice that the control and state trajectories are almost identical in all scenarios, apart from scenarios 4-5. In scenarios 4-5, the Feasible Direction Algorithm and the numerical solution of section 4.2 choose a different optimal control trajectory (therefore the speed trajectory is also different) due to the fact that the acceleration is negative. That means that the term of the total "tractive" force (R_T) in the fuel consumption model (see. section 2.5) is also negative for a long period of time, so the fuel consumption value is constant (equal to the idle fuel consumption α) and consequently the calculation of the gradient in the numerical algorithms is equal to zero. As far as, the difference between the values of the fuel consumption of each method, is concerned, the maximum percentage

difference is less than 2%, while in most scenarios and cases is less than 1%.

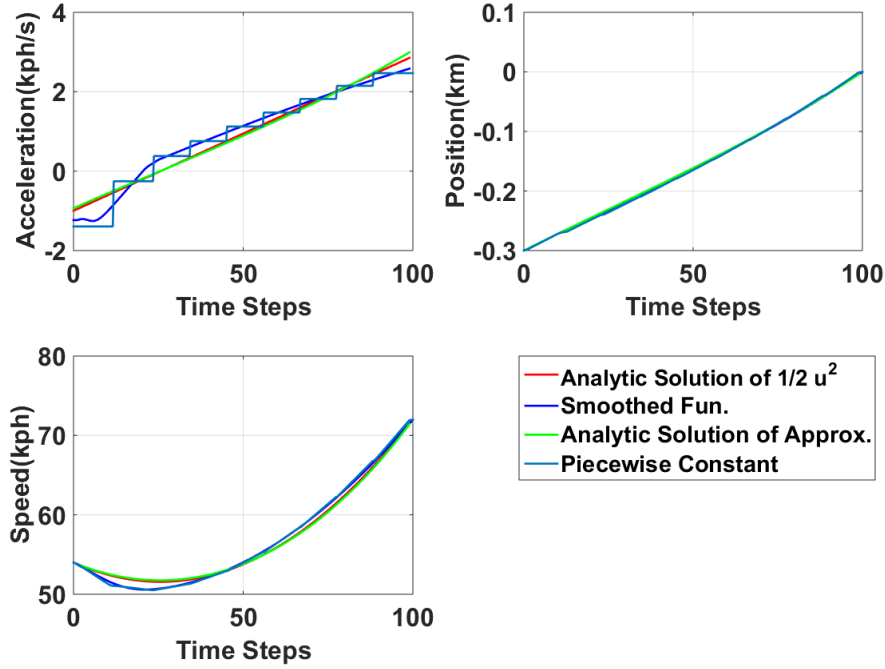


Figure 39: Comparison of control and states of analytic Solution of $\frac{1}{2}u^2$, smoothed function of ARRB fuel consumption model, Analytic Solution of the approximated model and piecewise constant method for Scenario 1

Results for $x_0 = -300$, $v_0 = 15$, $v_e = 20$	
	cost
Analytic Solution of $\frac{1}{2}u^2$	41.3356
Smoothed Function	41.4201
Taylor Approximation	41.7120
Piecewise Constant	41.6065

Table 10: Optimal fuel consumption of analytic solution of $\frac{1}{2}u^2$, smoothed function, analytic solution of the approximated model and piecewise constant method for Scenario 1

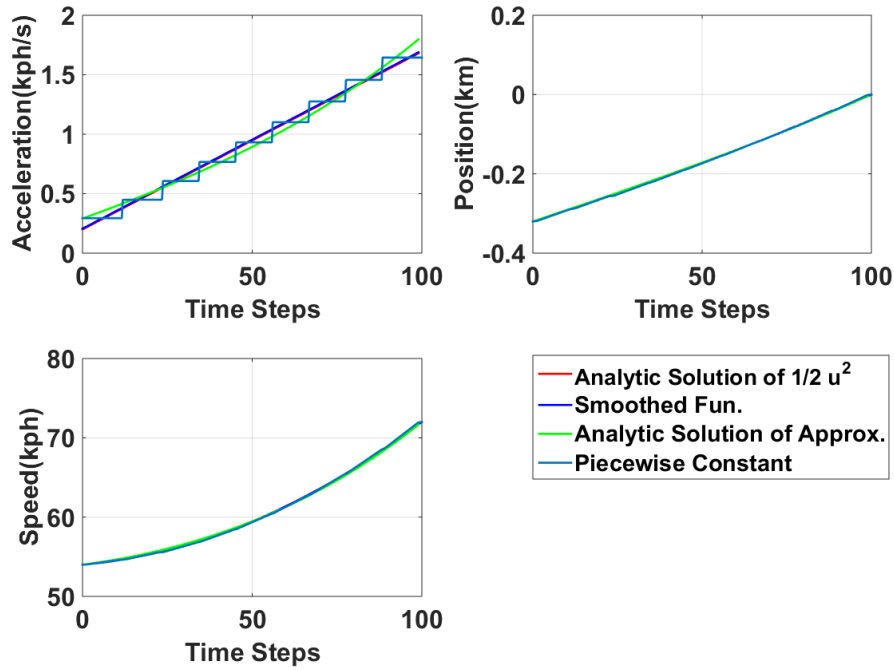


Figure 40: Comparison of control and states of analytic Solution of $\frac{1}{2}u^2$, smoothed function of ARRB fuel consumption model, Analytic Solution of the approximated model and piecewise constant method for Scenario 2

Results for $x_0 = -320$, $v_0 = 15$, $v_e = 20$	
	cost
Analytic Solution of $\frac{1}{2}u^2$	42.3915
Smoothed Function	42.0142
Taylor Approximation	42.1521
Piecewise Constant	42.1537

Table 11: Optimal fuel consumption of analytic solution of $\frac{1}{2}u^2$, smoothed function, analytic solution of the approximated model and piecewise constant method for Scenario 2

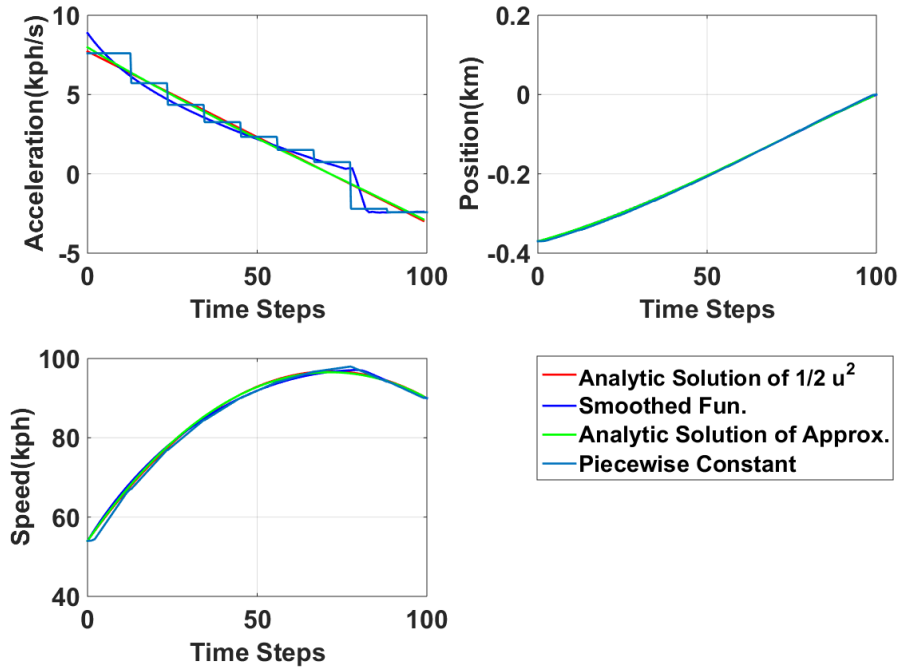


Figure 41: Comparison of control and states of analytic Solution of $\frac{1}{2}u^2$, smoothed function of ARRB fuel consumption model, Analytic Solution of the approximated model and piecewise constant method for Scenario 3

Results for $x_0 = -370$, $v_0 = 15$, $v_e = 25$	
	cost
Analytic Solution of $\frac{1}{2}u^2$	83.6274
Smoothed Function	82.0533
Taylor Approximation	82.9004
Piecewise Constant	82.7019

Table 12: Optimal fuel consumption of analytic solution of $\frac{1}{2}u^2$, smoothed function, analytic solution of the approximated model and piecewise constant method for Scenario 3

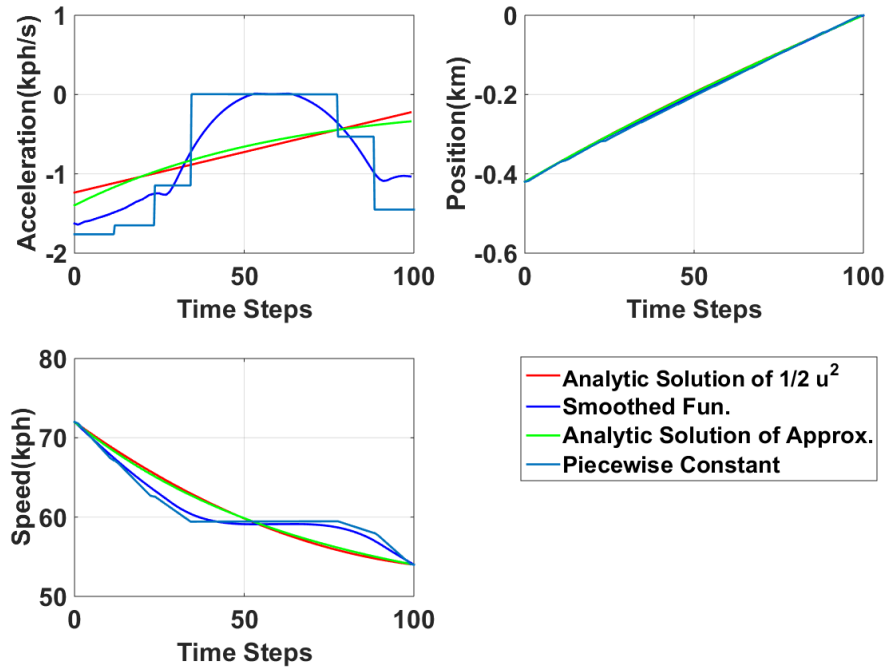


Figure 42: Comparison of control and states of analytic Solution of $\frac{1}{2}u^2$, smoothed function of ARRB fuel consumption model, Analytic Solution of the approximated model and piecewise constant method for Scenario 4

Results for $x_0 = -420$, $v_0 = 20$, $v_e = 15$	
	cost
Analytic Solution of $\frac{1}{2}u^2$	28.7724
Smoothed Function	28.7511
Taylor Approximation	28.7811
Piecewise Constant	28.7044

Table 13: Optimal fuel consumption of analytic solution of $\frac{1}{2}u^2$, smoothed function, analytic solution of the approximated model and piecewise constant method for Scenario 4

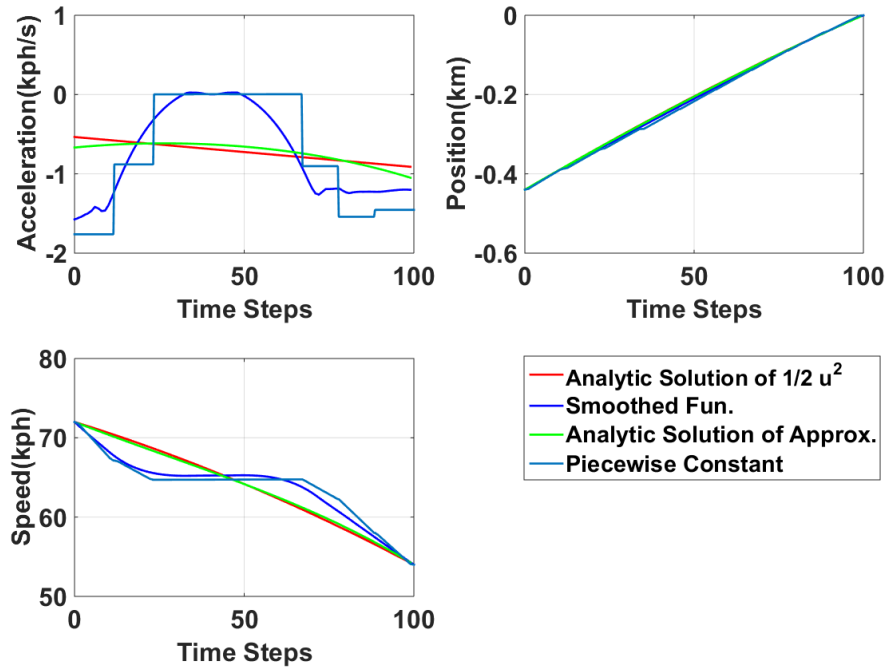


Figure 43: Comparison of control and states of analytic Solution of $\frac{1}{2}u^2$, smoothed function of ARRB fuel consumption model, Analytic Solution of the approximated model and piecewise constant method for Scenario 5

Results for $x_0 = -440$, $v_0 = 20$, $v_e = 15$	
	cost
Analytic Solution of $\frac{1}{2}u^2$	30.9743
Smoothed Function	30.8484
Taylor Approximation	30.8810
Piecewise Constant	30.7963

Table 14: Optimal fuel consumption of analytic solution of $\frac{1}{2}u^2$, smoothed function, analytic solution of the approximated model and piecewise constant method for Scenario

5

6

Maximisation Problem

At this final chapter, we introduce the maximisation of the cost function for our problem and then we compare the results with those of the minimisation problem. This results will show us the fuel consumption value range and also the effectiveness of the fuel consumption model approximation.

In order to take the maximum fuel consumption, we need to solve the following minimisation problem

$$\max(f(\mathbf{x})) \Leftrightarrow -\min(-f(\mathbf{x})) \quad (91)$$

subject to the state equations.

For the maximisation problem, we applied the constant control bound methodology (see section 2.4.4) for the acceleration and also added a penalty term for negative speeds in the objective function, in order to ensure that we will not have negative speed values.

$$\frac{1}{2} \min(0, v + \epsilon)^2 \quad (92)$$

So, in figures 44-46 and tables 15-17, we will present the comparison between the maximisation and minimisation problem of the smoothed ARRB fuel consumption model, for three of our scenarios, in respect to there control and states trajectories and their fuel consumption values.

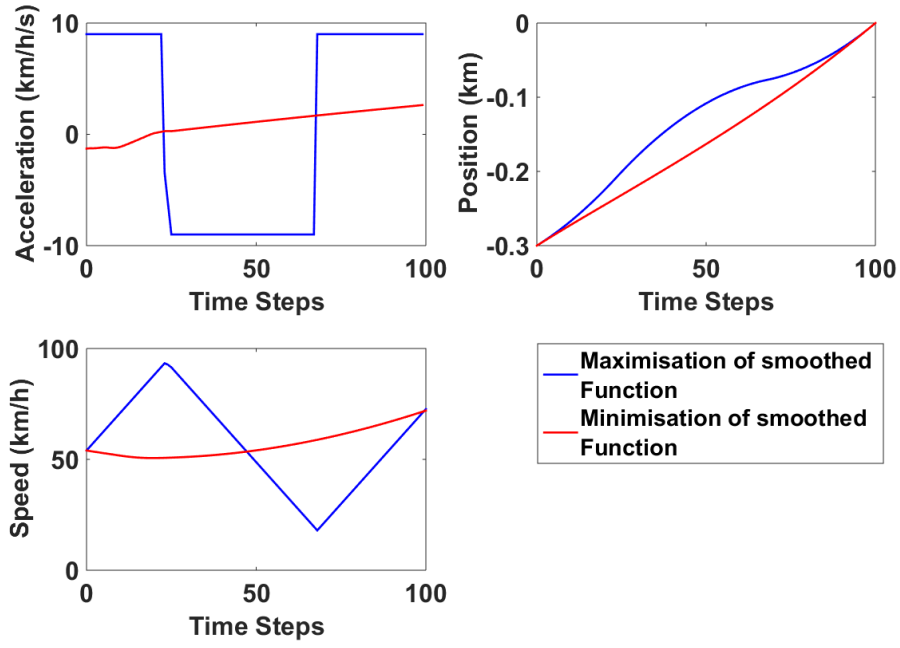


Figure 44: Comparison between minimisation and maximisation problem of the smoothed fuel consumption model for Scenario 1

	Maximisation of Smoothed Function	Minimisation of Smoothed Function	Difference
Cost Function Value	132.9080	41.4201	220%

Table 15: Maximum and minimum fuel consumption values of the smoothed fuel consumption model for scenario 1

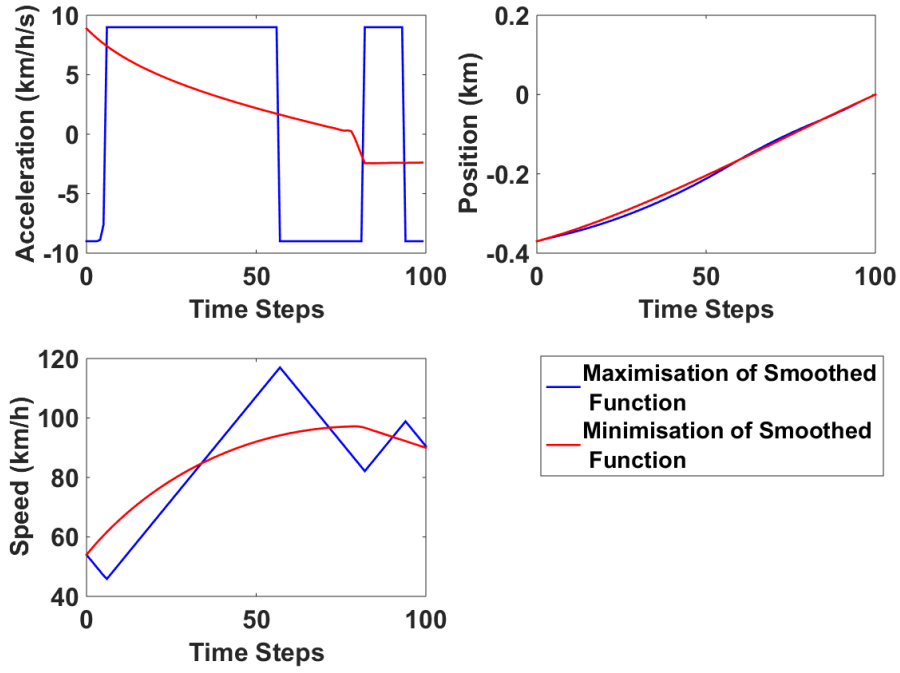


Figure 45: Comparison between minimisation and maximisation problem of the smoothed fuel consumption model for Scenario 3

	Maximisation of Smoothed Function	Minimisation of Smoothed Function	Difference
Cost Function Value	176.1853	82.0533	115%

Table 16: Maximum and minimum fuel consumption values of the smoothed fuel consumption model for scenario 3

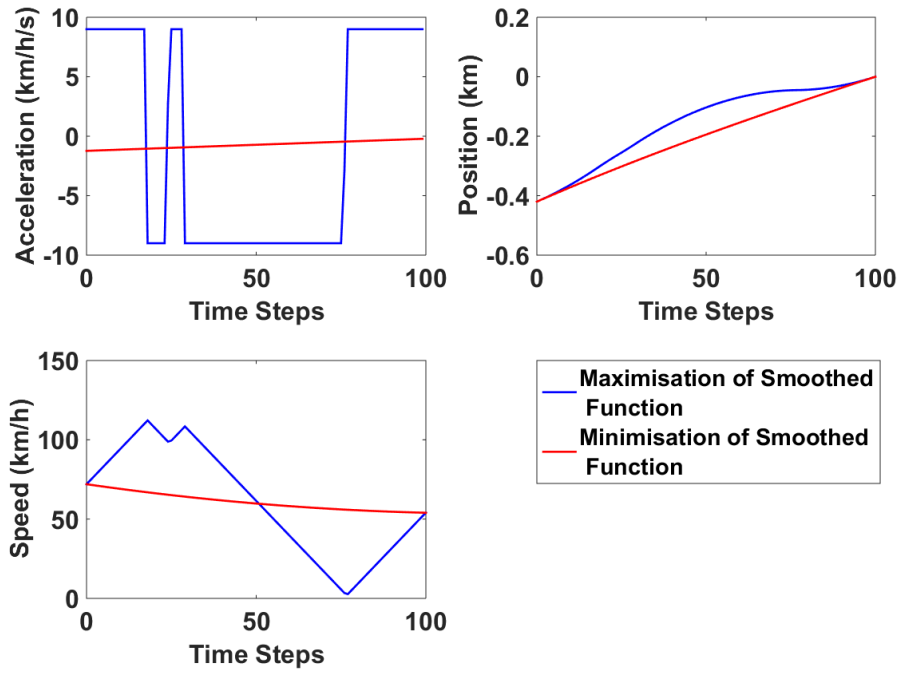


Figure 46: Comparison between minimisation and maximisation problem of the smoothed fuel consumption model for Scenario 4

	Maximisation of Smoothed Function	Minimisation of Smoothed Function	Difference
Cost Function Value	139.2375	28.7511	384%

Table 17: Maximum and minimum fuel consumption values of the smoothed fuel consumption model for scenario 4

7

Conclusions

The objective of this master thesis was the minimisation of the fuel consumption of a vehicle, by optimizing its trajectory (particularly its acceleration trajectory). In the first part, the fuel consumption problem formulated into an optimal control problem and solved, firstly, analytically (after an appropriate approximation) and then numerically. The results obtained from both solutions were quite satisfactory and the percentage difference between the two solutions was less than 3%. In the second part, the accuracy and the reliability of the fuel consumption problem was verified. In order to achieve this, firstly, a comparison of the results obtained from the cases where we set the same time horizon but different number of time steps was carried out. This comparison showed that there was a small loss of accuracy (less than 1%) from higher to smaller values of the number of time steps, which means that reasonably smaller number of time steps could be used in order to achieve less computational time of the fuel consumption problem. Secondly, the comparison of the results obtained from the cases where the time horizon differed and the time step was the same. From this comparison it would be shown, if the fuel consumption optimal problem is getting better as the algorithm has more options (more time) to lead the initial states to the final states. For limited time horizon, analytic solution and numerical solution gave almost the same trajectories and fuel consumption values but as the time horizon was increasing the fuel consumption values were close but the trajectories differed.

Afterwards the effectiveness of the fuel consumption model was validated. In this part, the maximisation of the fuel consumption problem was solved and compared the obtained results with those of the minimisation problem. Through these results, the value range of the fuel consumption model can be shown and with the percentage difference of the two solutions to be significantly large (more than 115%) it can be assumed that the fuel consumption model is quite efficient.

At the end, the fuel consumption problem was also solved by using as cost criterion the function $\frac{1}{2}u^2$ which is widely used in the bibliography for eco-driving problems and compared the results with those of the analytic and numerical solutions. The obtained results of trajectories and fuel consumption values was quite similar and the percentage difference of the fuel consumption value was less than 1% for all the cases, which lead us to the conclusion that using the function $\frac{1}{2}u^2$ is a good approach for eco-driving problems.

Bibliography

- Kyounggho Ahn, Hesham Rakha, Antonio Trani, and Michel Van Aerde. Estimating vehicle fuel consumption and emissions based on instantaneous speed and acceleration levels. *Journal of transportation engineering*, 128(2):182–190, 2002.
- Rahmi Akçelik and DC Biggs. Acceleration profile models for vehicles in road traffic. *Transportation Science*, 21(1):36–54, 1987.
- Todd M Bailey. Convergence of rprop and variants. *Neurocomputing*, 159:90–95, 2015.
- DP Bertsekas. Partial conjugate methods for a class of optimal control problems. *IEEE Transactions on Automatic Control*, Vol Ac-19, (3), 1974.
- DC Biggs. Estimating fuel consumption of light to heavy vehicles. Technical report, 1987.
- DC Biggs and R Akcelik. Validation of a power based model of car fuel consumption. 1984.
- DC Biggs and R Akcelik. Energy-related model of instantaneous fuel consumption. *Traffic Engineering and Control*, 27(6):320–325, 1986.
- DC Biggs and Rahmi Akçelik. Further work on modelling car fuel consumption. 1985.
- Darrell P Bowyer, Rahmi Akçelik, and DC Biggs. *Guide to fuel consumption analyses for urban traffic management*. Number 32. 1985.
- Arthur Earl Bryson. *Applied optimal control: optimization, estimation and control*. CRC Press, 1975.
- Alessandro Casavola, Giovanni Prodi, and Giuseppe Rocca. Efficient gear shifting strategies for green driving policies. In *American Control Conference (ACC), 2010*, pages 4331–4336. IEEE, 2010.

- David J Chang and Edward K Morlok. Vehicle speed profiles to minimize work and fuel consumption. *Journal of transportation engineering*, 131(3):173–182, 2005.
- Chunhui Chen and Olvi L Mangasarian. Smoothing methods for convex inequalities and linear complementarity problems. *Mathematical programming*, 71(1):51–69, 1995.
- Qi Cheng, Lydie Nouveliere, and Olivier Orfila. A new eco-driving assistance system for a light vehicle: Energy management and speed optimization. In *Intelligent Vehicles Symposium (IV), 2013 IEEE*, pages 1434–1439. IEEE, 2013.
- CIECA. Internal project on eco-driving in category b driver training & the driving test. final report, 2009. URL <http://www.thepep.org/ClearingHouse/docfiles/CIECA.internal.project.on.Eco-driving.pdf>.
- Imed Ben Dhaou. Fuel estimation model for eco-driving and eco-routing. In *Intelligent Vehicles Symposium (IV), 2011 IEEE*, pages 37–42. IEEE, 2011.
- Waleed F Faris, Hesham A Rakha, Raed Ismail Kafafy, Moumen Idres, and Salah Elmoselhy. Vehicle fuel consumption and emission modelling: an in-depth literature review. *International Journal of Vehicle Systems Modelling and Testing*, 6(3-4):318–395, 2011.
- Roger Fletcher. *Practical methods of optimization*. John Wiley & Sons, 2013.
- Elmer G Gilbert. Vehicle cruise: Improved fuel economy by periodic control. *Automatica*, 12(2):159–166, 1976.
- H Halkin, BW Jordan, E Polak, and JB Rosen. Theory of optimum discrete time systems. 1966.
- Erik Hellström, Maria Ivarsson, Jan Åslund, and Lars Nielsen. Look-ahead control for heavy trucks to minimize trip time and fuel consumption. *Control Engineering Practice*, 17(2):245–254, 2009.
- JN Hooker. Optimal driving for single-vehicle fuel economy. *Transportation Research Part A: General*, 22(3):183–201, 1988.
- Anahita Jamshidnejad, Hans Hellendoorn, Shu Lin, and Bart De Schutter. Smoothing for efficient solution of model predictive control for urban traffic networks considering endpoint penalties. In *Intelligent Transportation Systems (ITSC), 2015 IEEE 18th*

- International Conference on*, pages 2837–2842. IEEE, 2015.
- Md Abdus Samad Kamal, Masakazu Mukai, Junichi Murata, and Taketoshi Kawabe. Ecological vehicle control on roads with up-down slopes. *IEEE Transactions on Intelligent Transportation Systems*, 12(3):783–794, 2011.
- Apostolos Kotsialos and Markos Papageorgiou. Nonlinear optimal control applied to coordinated ramp metering. *IEEE Transactions on control systems technology*, 12(6):920–933, 2004.
- Sanjiban Kundu, Aditya Wagh, Chunming Qiao, Xu Li, Sandipan Kundu, Adel Sadek, Kevin Hulme, and Changxu Wu. Vehicle speed control algorithms for eco-driving. In *Connected Vehicles and Expo (ICCVE), 2013 International Conference on*, pages 931–932. IEEE, 2013.
- Andreas A Malikopoulos, Seongah Hong, Joyoung Lee, and Byungkyu Brian Park. Development and evaluation of speed harmonization using optimal control theory. *arXiv preprint arXiv:1611.04647*, 2016.
- Jerrold. E. Marsden and Anthony Tromba. *Vector Calculus*. Freeman, 1996.
- Ioannis A Ntousakis, Ioannis K Nikolos, and Markos Papageorgiou. Optimal vehicle trajectory planning in the context of cooperative merging on highways. *Transportation Research Part C: Emerging Technologies*, 71:464–488, 2016.
- M Papageorgiou and M Marinaki. A feasible direction algorithm for the numerical solution of optimal control problems. *Dynamic Syst. Simulation Lab., Tech. Univ. Crete, Chania, Greece*, 1995.
- Markos Papageorgiou. Certainty equivalent open-loop feedback control applied to multireservoir networks. *IEEE Transactions on Automatic Control*, 33(4):392–399, 1988.
- Markos Papageorgiou et al. *Optimierung*. Springer, 1991.
- J Pearson and R Sridhar. A discrete optimal control problem. *IEEE Transactions on automatic control*, 11(2):171–174, 1966.
- K Post, JH Kent, J Tomlin, and N Carruthers. Fuel consumption and emission modelling by power demand and a comparison with other models. *Transportation Research Part A: General*, 18(3):191–213, 1984.

Martin Riedmiller and Heinrich Braun. A direct adaptive method for faster backpropagation learning: The rprop algorithm. In *Neural Networks, 1993., IEEE International Conference on*, pages 586–591. IEEE, 1993.

Jo Bo Rosen. The gradient projection method for nonlinear programming. part i. linear constraints. *Journal of the Society for Industrial and Applied Mathematics*, 8(1):181–217, 1960.

Navteq Green Streets. White paper, 2009. URL <http://developer.navteq.com>.

Michael AP Taylor and Troy M Young. Fuel consumption and emissions models for traffic engineering and transport planning applications: some new results. In *COMBINED 18TH ARRB TRANSPORT RESEARCH CONFERENCE AND TRANSPORT NEW ZEALAND LAND TRANSPORT SYMPOSIUM, 2-6 SEPTEMBER 1996, CHRISTCHURCH, NEW ZEALAND PART 6*, 1996.

Hualiang Teng, Lei Yu, and Yi Qi. Statistical microscale emission models incorporating acceleration and deceleration. In *81st transportation research board annual meeting*, volume 29, 2002.

Joeri Van Mierlo, Gaston Maggetto, Erik Van de Burgwal, and Raymond Gense. Driving style and traffic measures-influence on vehicle emissions and fuel consumption. *Proceedings of the Institution of Mechanical Engineers, Part D: Journal of Automobile Engineering*, 218(1):43–50, 2004.